# 18. CALCAREOUS NANNOFOSSILS FROM THE SOUTHWEST PACIFIC, DEEP SEA DRILLING PROJECT, LEG 21

Anthony R. Edwards, New Zealand Geological Survey, Lower Hutt, New Zealand

## INTRODUCTION

This report is divided into two parts. The first part gives information on the overall nature, paleoenvironmental implications, and biostratigraphy of the calcareous nannofossils identified from the first three sites drilled on Leg 21. The second part deals with some of the main biostratigraphic, paleoecologic, and taxonomic conclusions reached as a result of this leg, which was the first warm-water marginal-sea cruise by the DV *Glomar Challenger*.

The Leg 21 sites can be readily subdivided into three groups which are distinctive in geography (Figure 1), geology, and calcareous nannofossil content (Table 1). The general characteristics of these groupings are as follows:

1) Sites 203 to 205 are located in the eastern part of the Fiji Sea *sensu lato* and are close to the western margin of the deep-sea Southwest Pacific Basin. They have essentially tuffaceous sequences directly related to the modern pattern of sea floor spreading and contain (Sites 203 and 205) warm oceanic Oligocene to Recent calcareous nannofossil assemblages fairly easily correlated with the low- to mid-latitude zonal schemes of the northern hemisphere. Sites 203, located at 22°09.22'S, 177°32.77'W and in 2720 meters of water, was cored sporadically to a maximum penetration of 409 meters. Site 204, at 24°57.27'S, 174°06.69'W with a water depth of 5354 meters, had a maximum penetration of 160 meters with semicontinuous coring. Site 205, at 25°30.99'S, 177°53.95'E with a water depth of 4320 meters, had a maximum penetration of 355 meters with continuous to semicontinuous coring.

2) Sites 206 to 208 are located in the northwestern part of the Tasman Sea adjacent to the deep-sea Tasman Basin. They have biogenic sequences which essentially contain warm becoming coolish oceanic latest Cretaceous to Recent nannofloras more readily correlated with their equivalent mid-latitude New Zealand assemblages than with those in the other Leg 21 sequences. Site 206, at 32°00.75'S, 165°27.15'E and a water depth of 3196 meters, had a maximum penetration of 734 meters with continuous to semicontinuous coring. Site 207, at 36°57.75'S, 165°26.06'E and in 1389 meters of water, had a maximum penetration of 513 meters with continuous coring. Site 208, at 26°06.61'S, 161°13.27'E, in 1545 meters of water, had a maximum penetration of 594 meters with semicontinuous coring.

3) Sites 209 and 210 are located in the Coral Sea, the first being marginal to, and the other within, the deep-sea Coral Sea Basin. They both have largely terrigenous sequences which contain warm neritic to oceanic mid Eocene to Recent nannofloras. The Paleogene assemblages are intermediate between those further south and north

whereas those from the Neogene are, in theory at least, readily correlatable with the equivalent Fiji Sea assemblages. Site 209, at 15°56.19'S, 152°11.27'E and in a water depth of 1428 meters, had a maximum penetration of 344 meters and was continuously cored. Site 210 at 13°45.99'S, 152°53.78'E and in a water depth of 4643 meters, had a maximum penetration of 711 meters with semicontinuous coring.

As indicated above, detailed initial reports are provided below for Sites 203 to 205. It was hoped that similar reports for the other sites could be given. However, the unexpectedly large amounts of material recovered from the Tasman Sea sites, 206 to 208, plus the need to document the regional unconformities discovered on Leg 21 have made this impossible in the time available. Consequently, the reports on Sites 206 to 210 will have to appear at a latter date. However, a moderately detailed report has been provided for the Site 209 sequence (see Chapter 9), and similar reports have been given for parts of three other sequences.

The shipboard observations were mainly made on core catcher samples because much of the writer's time was devoted to sampling (about 1400 samples, approximately 1 per meter of recovered core) and preparing simple cover glass strew mounts of the samples. Shore laboratory investigations were limited, in most cases, to a maximum of 15 minutes per sample; consequently, only the more conspicuous or significant taxa were identified. Even so, because of time limitations, it was found necessary to leave many of the samples unidentified beyond a brief examination to confirm their similar content and preservation to the overlying and underlying samples. All of the available samples from Sites 203 and 204 were examined in adequate detail as were all but a few of those from Sites 205 and 209.

## SITE 203

### Site Summary

This site (Figure 2), chosen to provide the age and composition of the Lau Basin interarc sediments, is located near the margin of a sediment pond which, for this area, is anomalously large, thick, and little disturbed. One hole, 203 (409 meters penetration, 5 cores cut, 20.3 meters recovery plus several meters of "supplementary sample"), was drilled at 22°09.22'S, 177°32.77'W in a water depth of 2730 meters.

The sequence encountered proved to be formed essentially of varying mixtures of nannofossil ooze and glass shard ash with the latter dominant except in the near-surface sediments. Unstable hole conditions forced
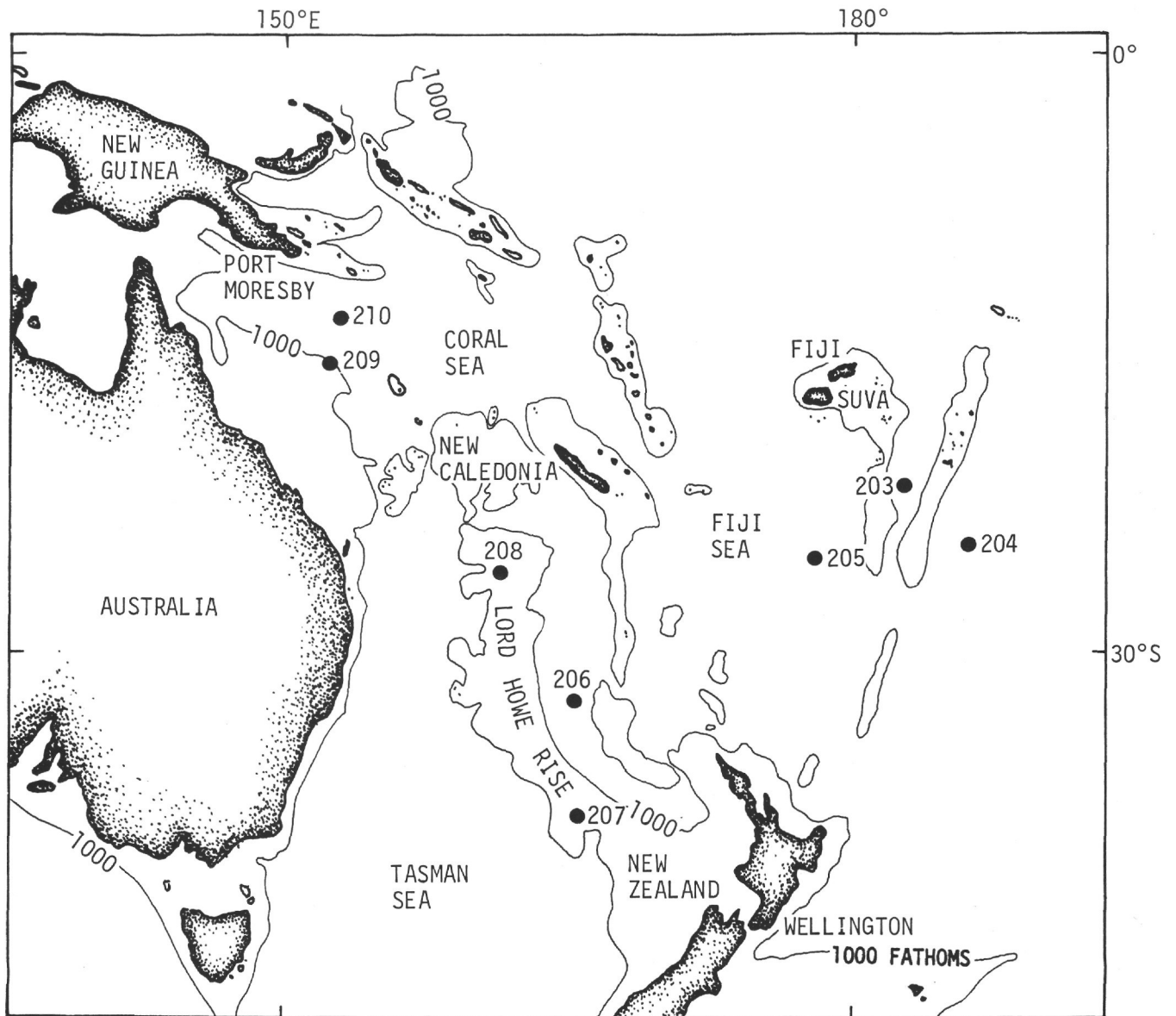
Figure 1. *Leg 21 site locations and track.*

abandonment prior to reaching acoustic basement (about 550 meters).

## Results and Comments

Cores 1 and 2, obtained between 0 and 15 meters below the sea floor (with 5.4 m and 2.0 m recovery respectively), consist of iron oxide rich nannofossil ooze with two thin intercalations of glass shard ash. Both cores are characterized by very abundant, diverse, and well-preserved calcareous nannofloras, but the overall calcareous nannofossil frequency is much lower in the strongly volcanogenic horizons (Table 2; for an explanation of the symbols used see Table 3).

The highest sample examined, some 15 cm below the top of Core 1, contains a nannoflora conforming to the "late" Pleistocene 3/3 *Emiliania huxleyi* (NN21) Zone of Martini (1971), which, according to McIntyre (1970), spans the last 250,000 years. A number of the taxa identified

from this assemblage have been recorded, by Norris (1961) and McIntyre et al. (1970), as living in this region. Interestingly, comparison of the relative frequencies of these taxa in this sample with the ecological data given in the latter paper suggests deposition from a marginally tropical (excluding equatorial) oceanic near-surface water mass slightly cooler than that occupying this region today (Stanton, 1969). The difference could well have resulted from annual variations of the type shown by Berger (1971, fig. 2).

The underlying seven samples from Cores 1 and 2 contain assemblages which are correlated with the Pleistocene 2/3 *Gephyrocapsa oceanica* (NN20) Zone of Martini (1971). This correlation is accepted despite the anomalous (reworked) occurrence of *Pseudoemiliania lacunosa* and questionable *Cyclococcolithina macintyrei*. Significantly, the highest numbers of *P. lacunosa* occur within and immediately above ash beds in Core 1. These beds could

TABLE 1
Calcareous Nannofossil Correlations, Leg 21 Sequences[a]

| Area and Site | | Coral Sea | | Tasman Sea | | | Fiji Sea | | |
|---|---|---|---|---|---|---|---|---|---|
| Adopted Age | | 210 | 209 | 208 | 206 | 207 | 205 | 203 | 204 |
| Pleistocene | | 1-12 | 1-3 | 1-2 | 1-11 | 1-4 | | 1-3 | |
| Pliocene | Late | 12-19 | 3-5 | 3-6 | 11-17 | 4-5 | | 4-5 | |
| | Early | 20-24 | ///// | 7-10 | 18-21 | 5-8A | 3 | | |
| Miocene | Late | 24-30 | ///// | 10- | 21- | | 3-8 | | |
| | Mid | 30-33 | 6 | | | 8A-10A | 10-24 | | |
| | Early | 33 | 10-12 | -25 | -6C | ///// | ///// | | |
| Oligocene | Late | 33? | 13-14 | 25-27 | 7C-15C | ///// | 24-29 | | |
| | Mid | 33 | ///// | | | ///// | 30 | | |
| | Early | 34? | ///// | ///// | ///// | ///// | | | |
| Eocene | Late | 35 | 15-27 | ///// | ///// | 9A | | | |
| | Mid | 36-46 | 28-34 | 27-29 | 15C-19C | 11A-23A | | | |
| | Early | 46-50 | | ///// | 19C | 24A-26A | | | |
| Paleocene | Late | | | ///// | ///// | 26A | | | |
| | Mid | | | 29 | 21C | 27A | | | |
| | Early | | | 29-33 | 19C-21C | 28A | | | |
| Maastrichtian | | | | 33-34 | | 28A? | | | 4-5, |
| Campanian | | | | | | | | | 1A |

[a]Entries are core numbers, cross-hatched areas are substantial disconformities, and heavy lines are the bases of the drilled sequence.

well have been deposited by bottom currents which had eroded and exposed older sediments. Use of a paleoenvironmental procedure similar to that outlined above gives results suggesting deposition of the *G. oceanica* Zone at this locality from a warm subtropical oceanic near-surface water mass. However, the extreme scarcity of *Coccolithus pelagicus* in this zone, and indeed in this sequence, suggests deposition some considerable distance from a temperate regime.

Core 3, from 108 to 117 meters (9.0 m recovery), consists of a massive glass shard ash underlain by a thinner impure nannofossil ooze. It contains common (in the ash) to abundant (in the ooze) moderately well preserved and fairly diverse nannofloras which, despite the sporadic occurrence of rare discoasters, are correlated with the Pleistocene 1/3 *Pseudoemiliania lacunosa* (NN19) Zone of Martini (1971). The occurrence of both forms of *P. lacunosa* in abundance and of possible *C. macintyrei* suggests a position moderately low (approximately Nukumaruan?) in this zone. Deposition appears to have been from a warm subtropical oceanic near-surface environment.

Core 4, from 229 to 238 meters (2.4 m recovery), consists of closely intercalated glass shard ash and impure nannofossil ooze horizons containing common moderately

well preserved fairly diverse nannofloras throughout. These assemblages are here correlated with the Late Pliocene 3/3 *Discoaster brouweri* (NN18) Zone of Martini (1971) despite the presence of rare specimens of *D. pentaradiatus* and battered *D. surculus* in the core catcher. It is worth noting that some of the specimens of *D. brouweri* in the Section 1 sample are also battered.

Core 5, from 400 to 409 meters (1.5 m recovery), consists of volcanogenic sand (downhole contamination?) underlain by glass shard ash horizons, two rounded vesicular basalt cobbles, and a lense of clay-rich nannofossil ooze. The latter and the core catcher sample contain abundant poorly preserved diverse assemblages which include many small specimens not identified in this cursory report. Both samples conform to the Late Pliocene 1/3 *Discoaster surculus* (NN16) Zone of Martini (1971). The presence of *Ceratolithus rugosus* in the core catcher sample suggests, according to Martini (1971, p. 769), that it comes from the lower part of this zone, i.e., from lowest part of the Late Pliocene *sensu* calcareous nannofossils.

The "supplementary sample", taken while trying to free the bottom hole assembly after Core 5 was obtained, consists of black volcanic sand very similar to that at the top of Core 5. It was sampled, at 34 cm in Section 1, to give an indication of the amount and nature of the
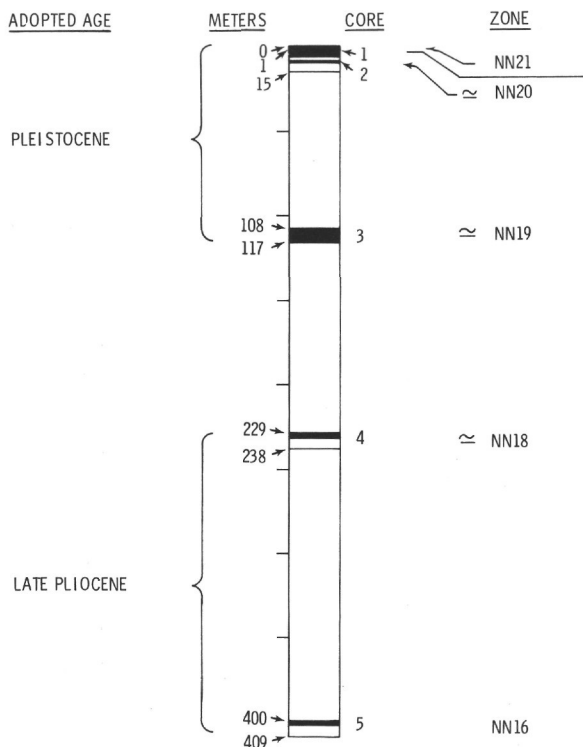
Figure 2. *Biostratigraphy of Site 203 as deduced from the calcareous nannofossils.*

downhole contamination present and thus of the background contamination likely to be encountered in the other holes. The calcareous nannofossils were found to be common and moderately well preserved with species present which clearly came from sediments near both the top and base of this hole. Some taxa, the discoasters, for example, may be penecontemporaneous with the sand but others, notably *Gephyrocapsa caribbeanica*, clearly are present as a direct result of the injection of drilling mud into this very porous sample.

The following depositional rates, uncorrected for compaction, can be calculated from the calcareous nannofossil biostratigraphy as matched to the time scale by Bukry (1971) and McIntyre (1970):

| Interval | Deposition rate (m/m.y.) |
|---|---|
| NN21 Zone | ~5 |
| Pleistocene | 65 to 130 |
| Site 203 | 110 |

These figures suggest a dramatic slowdown in the depositional rate during the latter part of the Pleistocene, a conclusion consistent with the observed lithologic changes. However, for technical reasons, there is no guarantee that the total thickness of the NN21 Zone in this area was recovered in full. Extrapolation of the overall depositional rate given above down to acoustic basement suggests that sedimentation at Site 203 began close to the Miocene-Pliocene boundary. Judging from the overall nature of the assemblages, the minimal corrosion observed, and the low

numbers of nannoliths, deposition was at depths similar to that at Site 203 today.

### Synopsis

At Site 203, in the southern part of the Lau Basin, common to abundant well-preserved diverse calcareous nannofloras indicative of warm subtropical to tropical oceanic conditions were deposited, together with large amounts of volcanogenic debris, at intermediate depths during earliest Late Pliocene to "late" Pleistocene time. Sedimentation at Site 203 may have commenced late in the Late Miocene.

## SITE 204

### Site Summary

This site, conspicuous among those drilled on Leg 21 due to the extreme scarcity of biogenic calcite, was selected to provide a biostratigraphy of the Pacific crustal sequence now being subducted into the nearby Tonga Trench. Two holes, 204 (150 m penetration, 9 cores cut, 49.4 m recovery) and 204A (95 m penetration, 1 core cut, 4.3 m recovery) were drilled at 24°57.27'S, 174°06.69'W in an uncorrected water depth of 5364 meters.

The 150-meter sequence encountered was comprised of 103 meters of abyssal silty clay, glass shard ash, and iron oxide clay abruptly underlain by 47 meters of tuffaceous sandstone and conglomerate. Basement (400 m plus?) was not reached.

### Results and Comments

The only calcareous nannofossils found at this site, which is at present well below the calcium carbonate compensation depth (CCD), occur in thin calcic silty clay horizons present in Cores 4 and 5 of Hole 204 and Core 1 of Hole 204A. Even in these horizons, which occur in the lower 13 meters of the abyssal clay unit, the nannofloras are very small, have very limited diversity and, although containing moderately well preserved taxa, also persistently contain strongly corroded coccolith remnants (Table 4).

The association of *Arkhangelskiella cymbiformis, Watznaueria barnesae,* and *W. paenepelagica* in this interval suggests that it is of Late Campanian or Early Maastrichtian age according to data presented by Bramlette and Martini (1964), Bukry (1969), and Manivit (1968) supplemented by the absence of *Watznaueria* in the Late Maastrichtian strata of the New Zealand region (including Hole 207) and Hole 208 (writer's observations). However, these age considerations should be treated with caution, if for no other reason than that no other similarly composed assemblage has yet been described from the southern hemisphere. Furthermore, the presence within this interval of radiolarians and arenaceous foraminifera considered to be of Oligocene or Early Miocene age (see site report) implies that the calcareous nannofossils are reworked.

If this is so, the most probable source of the reworking would be the northwestern part of the Louisville Ridge which, according to Hayes and Ewing (1971), is probably related to the northwesterly extension of the Eltanin

**TABLE 2**
Distribution of Calcareous Nannofossils, Site 203

Header interpretation (top rows, left→right across the data columns):

- **Adopted Age:** Pleistocene (Cores 1–3); Late Pliocene (Cores 4–5). (right margin: See text)
- **Adopted Zone:** NN21 | ~NN20 | ~NN19 | ~NN18 | ? | NN16
- **Lithologic Unit:** Nannofossil Ooze | Ash | Nanno Ooze | Ash and Nanno Ooze
- **Depth Below Sea Floor (m):** 0–6 | 6–15 | 108–117 | 229–238 | 400–409

| Taxon | C1-1 | C1-2 | C1-3 | C1-4 | C1-CC | C2-1 | C2-2 | C2-CC | gap | C3-1 | C3-2 | C3-3 | C3-4 | C3-5 | C3-6 | C3-CC | gap | C4-1 | C4-2 | C4-CC | gap | C5-1 | C5-CC | Supp |
|---|---|---|---|---|---|---|---|---|---|---|---|---|---|---|---|---|---|---|---|---|---|---|---|---|
| **Core** | 1 | 1 | 1 | 1 | 1 | 2 | 2 | 2 | | 3 | 3 | 3 | 3 | 3 | 3 | 3 | | 4 | 4 | 4 | | 5 | 5 | |
| **Section** | 1 | 2 | 3 | 4 | CC | 1 | 2 | CC | | 1 | 2 | 3 | 4 | 5 | 6 | CC | | 1 | 2 | CC | | 1 | CC | Suppl. |
| **Depth in Section (cm)** | 60 | 70 | 70 | 65 | | 90 | 70 | | | 70 | 65 | 70 | 70 | 70 | 70 | | | 75 | 43 | | | 106 | | |
| Ceratolithus cristatus | F | R | R | R | | R | R | R | | R | | R | R | R | R | R | | | R | | | | | r |
| Cyclococcolithina leptopora[a][b] | F | R | R | R | R | R | F | | | R | F | R | | R | R | R | | R | R | R | | | | r |
| Cyclolithella annula | R | R | F | | | | | | | | | | | | | | | | | | | | | |
| Discolithina japonica | R | R | R | | | | R | | | R | | | R | | R | R | | | | | | | | r |
| Emiliania huxleyi[a] | D | | | | | | | | | | | | | | | | | | | | | | | |
| Gephyrocapsa caribbeanica group | A | D | D | D | D | D | D | D | | | | | | r | | | | | | | | | | a |
| Gephyrocapsa oceanica[a] | C | | R | R | R | | R | | | | | | | | | | | | | | | | | |
| Helicopontosphaera[c] | C | F | F | F | F | F | F | F | | F | C | C | F | R | C | C | | C | C | C | | C | C | f |
| Pontosphaera discopora group | R | R | R | R | R | R | R | C | | F | R | R | R | R | C | F | | R | R | F | | R | R | |
| Rhabdosphaera clavigera[a][d] | C | F | F | C | F | C | F | C | | C | R | R | F | R | C | C | | R | F | R | | | | f |
| Scapholithus fossilis | F | R | | | | R | F | R | | R | | | R | | | R | | R | | | | | | |
| "Scyphosphaera"[a] | R | R | | | | R | R | R | | R | | R | R | R | R | F | | R | R | R | | R | F | |
| Syracosphaera histrica | C | C | R | F | | R | F | C | | C | F | R | F | R | F | F | | F | R | R | | | | r |
| Thoracosphaera heimii | R | R | R | R | R | R | R | | | R | | R | | | | | | R | | | | R | | r |
| Thoracosphaera imperforata? | R | R | | | R | R | R | R | | R | | R | R | | R | R | | R | R | | | R | F | r |
| Umbellosphaera tenuis[d] | F | | | | | | | | | | | | | | | | | | | | | | | |
| Gephyrocapsa protohuxleyi? | | R | | R | R | | | | | | | | | | | | | | | | | | | |
| Coccolithus pelagicus | | | R | R | | | | | | | | | | | | | | R | | | | | | |
| Oolithotus antillarum | | | | R | | | R | | | | | | | R | | | | | | | | | | |
| Cyclococcolithina macintyrei[e] | | r | r | r | | | | | | C | R | F | F | F | F | F | | R | C | F | | C | C | r |
| Pseudoemiliania lacunosa (circular) | | | c | f | | r | r | | | A | A | A | C | C | D | A | | A | A | C | | A | C | r |
| Pseudoemiliania lacunosa (oval) | | r | a | r | | | | | | C | C | A | C | F | C | A | | C | A | C | | A | A | |
| Syracosphaera pulchra[a] | | | | | | | | | | | | | | | | R | | | | | | R | | F |
| Discoaster brouweri | | | | | | | | | | r | | r | | | r | | | F | C | F | | R | F | F |
| Ceratolithus primus | | | | | | | | | | | | | | | | | | | | | | R | | |
| Discoaster pentaradiatus | | | | | | | | | | r | | | | | | | | | r | | | R | F | r |
| Discoaster surculus | | | | | | | | | | | r | | | | | | | | r | | | F | R | r |
| Discoaster variabilis[f] | | | | | | | | | | | | | | | | | | | | | | F | F | |
| Sphenolithus abies | | | | | | | | | | | | | | | | | | | | | | F | F | r |
| Ceratolithus rugosus | | | | | | | | | | | | | | | | | | | | | | R | | |
| Sphenolithus neoabies | | | | | | | | | | | | | | | | | | | | | | | F | |
| **OVERALL FREQUENCY** | D | D | C | D | D | D | D | D | | C | C | C | C | C | A | A | | C | C | C | | A | A | C |
| **COCCOLITH PRESERVATION** | G | G | G | G | G | G | G | G | | G | M | M | M | M | M | M | | M | M | M | | P | P | M |

Note: See table 3 for an explanation of symbols.

[a]Recorded as living in this region by Norris (1961).

[b]Most specimens resemble *Cyclococcolithus leptoporus* variety B of McIntyre, Bé & Preikstas (1967).

[c]Imperforate (*H. hyalina*) and perforate (*H. kamptneri, H. sellii,* and *H. wallichii?*) forms range throughout interval sampled.

[d]Recorded as living in this region by McIntyre, Bé, and Roche (1970).

[e]Core 1 to 3 specimens perhaps better referred to *C. leptopora* s.l.

[f]Includes the subspecies *decorus* and *pansus*.

Fracture Zone. These authors also state that the crest of the ridge is often flattened, at approximately 1,500 meters, to an extent which suggests truncation. If the area around Site 204 has undergone overall deepening of the order of say 500 to 1000 meters at some time subsequent to the commencement of abyssal clay deposition at Site 204, it would explain the survival of the nannofossils in such a harsh depositional environment. Alternatively, their occurrence could be due to the calcium carbonate compensation depth formerly being deeper. Either way, their post-depositional survival is almost certainly due to the buffering effect of the associated "nonbiogenic" calcite which may have, in part or whole, been derived from reworking of the calcite veins in the underlying tuffaceous sandstones.

**TABLE 3**
Symbols Key for Tables 2, 4-8, 10-11

| Frequency | Symbol[a] |
|---|---|
| Dominant (over 50%) | D |
| Abundant | A |
| Common | C |
| Few | F |
| Rare | R |
| Very rare | V |
| Present (1-5 specimens) | X |

| Preservation[b] | Symbol |
|---|---|
| Good | G |
| Moderate | M |
| Poor | P |

[a]These symbols are in lower case when species are thought to be present due to reworking or contamination.

[b]Based on the coccolith (as distinct from the nannolith) content.

## Synopsis

At Site 204, on the western margin of the Pacific crustal plate, calcareous nannofossils are only present in the basal part of the abyssal clay unit. Even here they are represented by very sparse residual assemblages clearly deposited close to the calcium carbonate compensation depth. Although a definite Late Cretaceous, and a probable Late Campanian or Early Maastrichtian, age is indicated, other microfossil evidence suggests that these nannofloras are totally reworked.

## SITE 205

### Site Summary

This site (Figure 3), selected to provide a relatively thin but representative eastern South Fiji Basin sedimentary sequence, is located just west of the break in slope between the basin floor and the western flank of the Lau Ridge. One hole, 205 (355 m penetration, 32 cores cut, 134.7 m recovery), was drilled at 25°30.99'S, 177°53.95'E in a water depth of 4330 meters.

The semicontinuously cored sequence drilled is comprised of four lithologic units: (a) 20 to 35 meters of abyssal iron oxide clay, with minor nannofossil ooze in the lower part, grading rapidly down into (b) about 240 meters of glass shard ash and vitric tuff, with abundant nannofossil ooze intercalated in the upper 30 meters, underlain by 63 meters of nannofossil ooze, chalk, and limestone interbedded with zeolite and glass shard rich horizons and basally intruded by (d) 18 meters of basalt. Basement (about 565 m) was not reached.

### Results and Comments

Core 1, obtained between 0 and 9 meters below the sea floor, contained only a small lump of pumice.

Core 2, from 9 to 18 meters (7.3 m recovery), consists of glass-rich iron oxide clay which lacks calcareous nannofossils.

Core 3, from 18 to 27 meters and with a 7.7 meter recovery, contains intercalated iron oxide clay, iron oxide rich nannofossil clay, and iron oxide bearing nannofossil

**TABLE 4**
Distribution of Calcareous Nannofossils, Site 204

| Adopted Age | Oligocene or Early Miocene | | | | |
|---|---|---|---|---|---|
| Inferred Age | Late Campanian to Early Maastrichtian | | | | |
| Lithologic Unit | Abyssal clay | | | | |
| Hole | 204 | | | 204A | |
| Depth Below Sea Floor (m) | 85-94 | | 94-103 | 86-95 | |
| Core | 4 | | 5 | 1 | |
| Section | 4 | CC | CC | 3 | CC |
| Depth in Section (cm) | 145[c] | | top | 138[c] | |
| Corroded coccolith rims | R | R | R | R | |
| Micula staurophora [a] | R | R | | R | |
| Tetralithus obscurus? | R | R | | R | |
| Arkhangelskiella cymbiformis[b] | | R | X | R | |
| Deflandrius cretaceus[b] | | R | | R | |
| Watznaueria paenepelagica | | R | R | R | |
| Cribrosphaerella ehrenbergii | | | R | R | |
| Podorhabdus ? quadriperforatus | | | | X | |
| Watznaueria barnesae | | | | R | |
| OVERALL FREQUENCY | R | R | R | F | |
| COCCOLITH PRESERVATION | P | P | M | M | |

Note: See Table 3 for an explanation of symbols.

[a]Strongly calcified.

[b]Presence in 204-4, CC debatable.

[c]Samples 204-4-4, 145 cm and 204A-1-3, 138 cm are from closely similar stratigraphic levels.

ooze beds and lenses. Minor components include zeolites, glass shards, and foraminifera. Seven samples were examined (Table 5).

The highest sample, from Section 2 at 112 cm, contains an abundant diverse moderately well preserved residual assemblage which, besides obvious reworking from early Neogene sediments, includes taxa indicative of the Early Pliocene 2/4 *Ceratolithus rugosus* (NN13), Late Miocene 4/5 to 3/5 *Discoaster quinqueramus* (NN11), and Late Miocene 1/5 *Discoaster hamatus* (NN9) zones of Martini (1971). Also present by implication are taxa from Martini's intervening *Ceratolithus tricorniculatus* (NN12) and *Discoaster calcaris* (NN10) gap zones. The possibility that this situation resulted from disturbance during drilling seems slim as Core 3 does not appear to have suffered any more obvious deformation than is usual in surficial cores. Accordingly, the writer accepts the presence of very rare but well-preserved *C. rugosus* as in place and, since the younger species, *D. asymmetricus*, was not observed, this sample is considered to be a correlative of the Early Pliocene 2/4 *Ceratolithus rugosus* (NN13) Zone of Martini (1971). The presence of taxa indicative of older zones is attributed to substantial reworking. The nature of bottom topography of the area around Site 205 strongly suggests that the source of this reworking was the nearby north-south trending ridge which today represents the junction between the Lau Ridge and the South Fiji Basin.
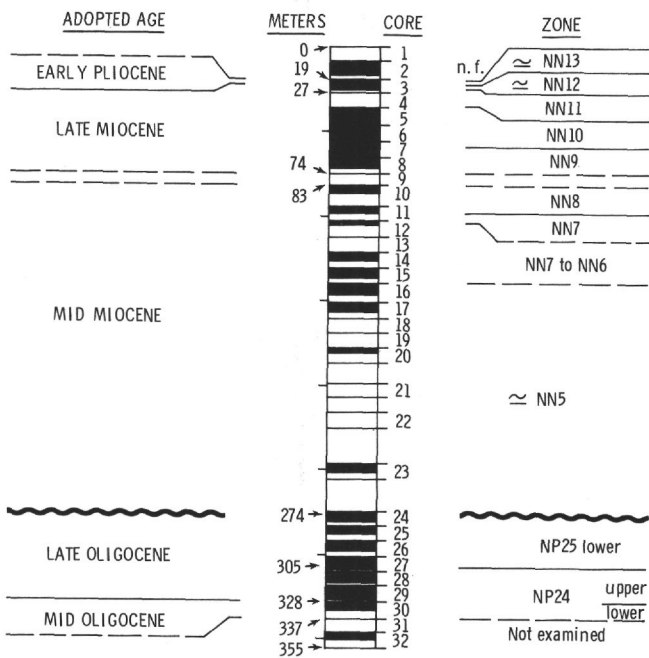
Figure 3. *Biostratigraphy of Site 205 as deduced from the calcareous nannofossils.*

Non-paleontologic considerations suggest (see the final Site 205 comments given below) that uplift occurred at this junction during the Late Miocene.

The middle samples, from Section 3 at 75 cm and Section 4 at 75 cm, contain nannolith-dominated residual nannofloras low in both diversity and abundance. The higher sample appears to be a correlative of the lower (Late Miocene 5/5) part of the *Ceratolithus tricorniculatus* (NN12) Zone of Martini (1971) since it lacks *C. amplificus, C. rugosus,* and *D. quinqueramus.* Because other members of *Ceratolithus* and *Discoaster* are present, it seems unlikely that their absence is due to solution effects. However, both this and the lower sample were clearly deposited very close to the lower limit of the calcium carbonate compensation level. This is especially true of the lower sample which, as a result, is hard to accurately locate biostratigraphically. Its grouping with either the Section 3 or Section 5 samples is dependent on the taxonomic interpretation placed on certain rare five-rayed discoasters lacking the axial part of their center. The writer suspects that these specimens are corroded *D. quinqueramus.* If this is so, the sample conforms to the *D. quinqueramus* (NN11) Zone of Martini (1971).

The lower samples, from Section 5 at 81 cm to the core catcher, contain common poorly to moderately well preserved residual nannofloras of low diversity. All contain substantial numbers of *D. quinqueramus* and thus conform to the *Discoaster quinqueramus* (NN11) Zone of Martini (1971) despite the presence of obvious reworking from older sediments. Placement of these samples within the subdivisions of this zone is more difficult due to the sporadic occurrence of *D. berggrenii.* Section 6 and the core catcher sample can, with reasonable confidence, be placed in the lower (Late Miocene 3/5) part of this zone. In contrast, the presence of very rare *D. berggrenii* in the

Section 5 sample could well be due to biological activity having caused vertical mixing in these very slowly deposited sediments (cf. Berger and Heath, 1968); the lithologic description of this part of the core is consistent with such an interpretation. Accordingly, the Section 5 sample is considered to be a probable correlative of the upper (Late Miocene 4/5) part of the *D. quinqueramus* Zone of Martini (1971).

Core 4, from 27 to 36 meters and with a core catcher recovery only, consists of glass shard, foraminifer-, and radiolarian-bearing clay nannofossil ooze and contains an abundant diverse moderately well preserved residual flora. Like the overlying basal Core 3 floras, this assemblage contains *Discoaster berggrenii* and *D. quinqueramus* without associated *C. amplificus* nor *C. rugosus.* Accordingly, despite the apparent presence of minor reworking from NN9 or NN8 zones and older sediments, the writer has no hesitation in correlating these floras with the lower (Late Miocene 3/5) part of the *Discoaster quinqueramus* (NN11) Zone of Martini (1971). In containing much clay and low amounts of glass shards, the sample is lithologically more similar to the overlying Core 3 than to the underlying Core 5. Thus, both the nannofossil and lithologic evidence suggest that the core catcher sample came from the upper part of the cored interval.

Cores 5 and 6, from 38 to 56 meters and with 9.2-meter recoveries in both cases, contain a number of alternations between impure nannofossil ooze and glass shard ash with the former lithology predominating. Small amounts of iron oxide occur in Section 1 to 4 of Core 5. Samples examined from these two cores yielded abundant (usually) to common low diversity moderately well preserved residual nannofloras. However, the assemblages of Core 5, Sections 2 to 5, include numerous discoasters with prominent calcite overgrowths which probably result from incipient diagenesis (Wise, 1972). All of the assemblages conform to the Late Miocene 2/5 *Discoaster calcaris* (NN10) Zone of Martini (1971) which he records from the stratotype Tortonian of Italy and the Upper Mohnian of California. The lowest sample is notable for the highest occurrences, apart from those probably due to reworking, of *Discoaster neohamatus* and *Reticulofenestra* n.sp.A. The latter is an undescribed medium-sized oval species having a broad "flat" central area with a central oval perforation. It was first recognized by the writer in the Late Miocene of New Zealand where it is widespread and has its highest occurrence high in the Kapitean Stage (latest Miocene?).

Cores 7 and 8, from 56 to 74 meters and with 9.0- and 6.2-meter recoveries, respectively, consist of variable impure (often radiolarian-rich) nannofossil ooze and nannofossil glass shard ash intercalations (Core 7) underlain by nannofossil glass shard ash with conspicious pumice (Core 8). These lithologies yielded common to abundant, poorly to moderately well preserved residual nannofloras which, apart from a diverse assemblage in the core-catcher of Core 8, have low diversities. The highest assemblage examined, from Section 1 of Core 7, is referable to the *D. calcaris* (NN10) Zone (for further data see above) whereas all the underlying floras conform to the Late Miocene 1/5 *Discoaster hamatus* (NN9) Zone of Martini (1971), which occurs in the Tortonian stratotype in Italy.

647

### TABLE 5
### Distribution of Calcareous Nannofossils, Cores 2-9, Site 205

| Row / Taxon | CC | 2 | 3 | 4 | 5 | 6 | CC | CC | 1 | 3 | CC | 3 | CC | 1 | 3 | 5 | CC | 2 | 3 | 5 | CC | |
|---|---|---|---|---|---|---|---|---|---|---|---|---|---|---|---|---|---|---|---|---|---|---|
| **Adopted Age** | Early Pliocene | Late Miocene → | | | | | | | | | | | | | | | | | | | | |
| **Adopted Zone** | NN13 | NN12 (lower) | NN11 (upper) | NN11 (lower) → | | | | | NN10 → | | | | | NN9 → | | | | | | | | |
| **Lithologic Unit** | Iron oxide clay and nannofossil ooze → | | | | | | | Glass shard ash and minor nannofossil ooze → | | | | | | | | | | | | | | |
| **Depth Below Sea Floor (m)** | 18-27 | | | | | | | 27-36 | 38-47 | | | 47-56 | | 56-65 | | | | 65-74 | | | | |
| **Core** | 2 | 3 | | | | | | 4 | 5 | | | 6 | | 7 | | | | 8 | | | | 9 |
| **Section** | CC | 2 | 3 | 4 | 5 | 6 | CC | CC | 1 | 3 | CC | 3 | CC | 1 | 3 | 5 | CC | 2 | 3 | 5 | CC | |
| **Depth in section (cm)** | 112 | 75 | 75 | 81 | 10 | | | | 40 | 25 | | 25 | | 84 | 25 | 25 | | 25 | 25 | 25 | | |
| *Acanthoica* | X | X | | | | | | | | | | X | X | | | | | | | | | |
| *Ceratolithus rugosus* | R | | | | | | | | | | | | | | | | | | | | | |
| *Ceratolithus tricorniculatus* | R | R | R | R | R | R | X | | | | | | | | | | | | | | | |
| *Coccolithus* cf. *pelagicus*[a] | F | R | R | C | R | F | F | R | R | C | R | R | R | | R | R | | R | F | C | F | |
| *Cyclococcolithina macintyrei* | C | R | | C | X | R | C | F | R | F | R | R | C | F | R | | | R | F | C | F | |
| *Discoaster brouweri* | C | R | R | R | | | C | C | R | C | F | C | F | | | | | | | | | |
| *Discoaster pentaradiatus* | F | X | X | | X | | C | C | | F | R | | | | | | | | | | | |
| *Discoaster surculus* | C | F | X | R | X | | R | R | | | | | | | | | | | | | | |
| *Discoaster variabilis* group[b] | C | R | C | A | | A | C | C | C | C | C | C | C | C | C | D | | A | A | C | R | |
| *Helicopontosphaera kamptneri* group | F | X | | X | | | X | C | R | | | R | F | C | R | F | | A | R | C | F | |
| *Reticulofenestra pseudoumbilica* | A | X | | F | | | C | R | R | | | F | F | F | R | R | R | R | C | A | C | |
| *"Scyphosphaera"*[c] | X | | | | | | X | | | | | | | X | | | | | | X | | |
| *Sphenolithus moriformis* group[d] | F | | | | | | R | | R | | | R | F | R | | | | | | F | R | |
| *Triquetrorhabdulus rugosus* | X | | | X | X | | R | R | X | | | | | R | | | | | | | | |
| *Discoaster quinqueramus* | f | | ? | F | C | C | F | | | | | | | | | | | | | | | |
| *Discoaster neorectus* | X | X | | X | X | | C | F | A | | | A | | | | | | | | | | |
| *Discoaster berggrenii* | | | | X | F | | F | R | | | | | | R | | | | | | | | |
| *Discolithina* (many pores) | | | | | | | X | | | | | | | | | | | | | X | | |
| *Discoaster neohamatus* | r | | | | | | r | | | | | | R | C | R | R | | F | | C | R | |
| *Reticulofenestra* n. sp. A (see text) | f | | | | | c | | | | | | | F | F | R | F | | F | | R | F | |
| *Cyclococcolithina rotula* | | | | | | | | | | | | | | R | | | | | R | | R | R |
| *Discoaster hamatus* | X | | | | | | | | | | | | | | F | F | | R | F | R | F | X |
| *Catinaster calyculus* | X | | | | | | | X | | | | | | | | F | F | C | C | F | C | |
| *Discoaster calcaris* | | | | | | | | | | | | | | | | F | R | R | | F | | C |
| *Catinaster coalitus* | | | | | | | | | | | | | | | | | | | | | | R |
| *Coccolithus eopelagicus* | | | | | | | | | | | | | | | | | | | | | | R |
| *Rhabdosphaera claviger* | | | | | | | | | | | | | | | | | | | | | | X |
| *Syracosphaera histrica* | | | | | | | | | | | | | | | | | | | | | | R |
| *Discoaster deflandrei* | | X | | r | | | X | | | | | | | | | | | | | | | r |
| *Cyclicargolithus floridanus* | c | | | | | | r | | | | | | | | | | | | | | | r |
| *Helicopontosphaera euphratis* | | | | | | | | | | | | | | | | | | | | | | X |
| **OVERALL FREQUENCY** | — | A | F | F | C | C | C | A | C | A | C | A | A | A | C | C | A | A | A | A | C | |
| **COCCOLITH PRESERVATION** | — | M | M | P | M | M | P | M | M | M | M | M | M | M | P | M | P | P | M | P | P | |

Note: See Table 3 for an explanation of symbols.

[a]Includes *Ericsonia ovalis*, etc.

[b]Includes *D. intercalaris*.

[c]Often strongly corroded. Includes *Crassapontosphaera* Boudreaux and Hay.

[d]Includes *S. neoabies*, *S. pacificus*, etc.

Core 9, from 74 to 83 meters, was retrieved empty.

Cores 10 and 11, from 83 to 104 meters and with 3.1- and 3.7-meter recoveries, consist of nannofossil glass shard ash (Core 10) underlain by a 1.1-meter bed of glass nannofossil ooze and further nannofossil-rich glass shard ash, all of which are semi-indurated. The nannofloras comprise common to abundant, fairly diverse, moderately (usually) to poorly preserved residual assemblages (Table 6).

The Core 10 and Core 11, Section 3, assemblages can be definitely placed in the mid-Miocene 4/4 *Catinaster coalitus* (NN8) Zone of Martini (1971). The presence of single specimens of *Sphenolithus heteromorphus* and *Discoaster deflandrei* in the Core 10, Section 1 assemblage examined clearly can be attributed to reworking from NN5 (mid-Miocene 1/4) to NN3 (Early Miocene 3/4) strata.

The Core 11 core catcher assemblage is very similar to the above assemblages but lacks *C. coalitus* and consequently, on the grounds of sequential position and probable depositional continuity, can with reasonable confidence, be correlated with the mid-Miocene 3/4 *Discoaster kugleri* (NN7) Zone of Martini (1971) despite the absence of the name bearer which is also the index species.

Cores 12, 13, and 14, from 104 to 131 meters and with 1.0-meter, core catcher only, and 4.7-meter recoveries, respectively, consist of semi-lithified nannofossil-bearing glass shard, ash, and vitric tuff. The nannofloras are comprised of very rare to rare, poorly preserved (battered) residual assemblages with very low to low diversity. Although obviously of mid Miocene age, these assemblages cannot, at present, be more accurately dated on their content alone despite the highest occurrences of *Cyclicargolithus floridanus* and *Discoaster exilis* within this interval, which also contains the lowest recognized occurrence of the *D. variabilis* group. Accepting their rather uncertain sequential position (see below), these floras are considered a correlative of the combined mid Miocene 3/4 and 2/4 *Discoaster kugleri* (NN7) and *Discoaster exilis* (NN6) zones of Martini (1971).

Cores 15, 16, and 17, from 131 to 160 meters and with 5.4-, 6.8-, and 5.5-meter recoveries respectively, consist of semi-lithified nannofossil-bearing to nannofossil-rich vitric tuff, often mottled, with a thin bed, in Section 5 of Core 17, of poorly sorted lithic lapilli tuff. The Core 15 assemblages are very similar to those of the three overlying cores and are datable on identical grounds (see above). In contrast, the underlying assemblages of Cores 16 and 17 are, for no obvious lithologic reason, distinctly better, being represented by common diverse poorly preserved, but not battered, residual floras. This is particularly the case in the Core 16, Section 3 sample examined, which clearly can be correlated with the mid Miocene 1/4 *Sphenolithus heteromorphus* (NN5) Zone of Martini (1971) because it contains both the name bearer and *D. exilis*. This zone occurs in the Langhian stratotype according to Martini (1971, p. 765). The underlying assemblages of Cores 16 and 17 can also be correlated with the *S. heteromorphus* (NN5) Zone on the grounds of sequential position together with the presence of *D. exilis*.

Core 18, from 160 to 169 meters, was retrieved empty.

Cores 19 through 23 have the following physical characterics (all figures are in meters):

| Core | Depth | Recovery | Lithology |
|------|-------|----------|-----------|
| 19 | 169-178 | minor | Nanno-rich glass shard ash. |
| 20 | 178-187 | 2.0 | Glass shard ash and nanno vitric tuff. |
| 21 | 198-207 | CC only | Nanno-bearing ash. |
| 22 | 216-225 | CC only | Nanno-rich ash. |
| 23 | 246-255 | 6.2 | Mottled vitric and lithic lapilli tuff underlain by glass-bearing nanno ooze. |

As might be expected from these lithologies, the nannofossil content, diversity, and, to a lesser degree, preservation vary greatly, particularly in Core 23 (Table 7). A number of taxa have their lowest occurrence within this interval, but, despite this, the biostratigraphic position can at present only be inferred, for the same reasons as given above and below, as probably correlative with the mid-Miocene 1/4 *Sphenolithus heteromorphus* (NN5) Zone of Martini (1971). The occurrence of rare *Triquetrorhabdulus carinatus* in the core catchers of Cores 20 and 22 indicates reworking from Late Oligocene or Early Miocene strata.

Core 24, from 274 to 283 meters and with 5.0 meters recovery, consists of about 1 meter of intensely burrowed nannofossil vitric tuff, with a very thin sandy layer at the base, disconformably underlain, at 40 cm in Section 2, by intercalated beds of glass shard bearing nannofossil ooze, occasionally richly zeolitic, and zeolite- and nannofossil-bearing glass shard ash. The highest nannofossil sample taken, at 22 cm in Section 2, yielded a common moderately well preserved (but with "overcalcified" discoasters) residual assemblage of low diversity and similar to those of the overlying cores. Like the floras in those cores, this assemblage, in containing *D. exilis* (see Martini, 1971, p. 765) and underlying the Core 16 occurrence of *S. heteromorphus*, is a probable correlative of the mid Miocene 1/4 (Langhian) *Sphenolithus heteromorphus* (NN5) Zone of Martini (1971). However, since *D. exilis* is unlikely to have its first appearance exactly at the base of the zone, the possibility of correlation with the uppermost part of this underlying Early Miocene 4/4 *Helicopontosphaera ampliaperta* (NN4) Zone cannot be exluded. According to Martini (loc. cit.), the upper part of the latter zone is present in the lowest part of the stratotype of the Langhian Stage of Italy. No obvious reworking from the underlying sediments was observed.

The immediately underlying samples at 45 and 53 cm in Section 2, taken from the top of the highest Core 24 nannofossil ooze bed, contain abundant low-diversity poorly preserved residual nannofloras. These two assemblages, like those underlying, have a markedly different floral composition than that obtained from the highest Core 24 sample. This difference reflects not only the intervening abrupt lithologic change, but also a corresponding age jump from early mid Miocene above to latest Oligocene below. The latter age can be inferred from the presence in these samples of both the early Neogene species *Sphenolithus belemnos* and the late Paleogene index *Reticulofenestra bisecta*. As indicated elsewhere (see below), this overlap occurs very high in the Late Oligocene

**TABLE 6**
**Distribution of Calcareous Nannofossils, Cores 10-18, Site 205**

| | 10-1 (20) | 10-CC | 11-3 (25) | 11-CC | 12-1 (base) | 12-CC (105) | 13-CC | 14-2 (27) | 14-3 (20) | 14-CC | 15-1 (95) | 15-3 (25) | 15-CC | 16-3 (25) | 16-CC | 17-2 (68) | 17-5 (64) | 17-CC | 18 |
|---|---|---|---|---|---|---|---|---|---|---|---|---|---|---|---|---|---|---|---|
| **Adopted Age** | Mid Miocene | | | | | | | | | | | | | | | | | | |
| **Adopted Zone** | NN8 | | | | NN7 | NN7 to NN6 | | | | | | | | ~NN5 | | | | | |
| **Lithologic Unit** | Glass shard ash and minor nannofossil ooze | | | | | | | | | | | | | | | | | | |
| **Core** | 10 | 10 | 11 | 11 | 12 | 12 | 13 | 14 | 14 | 14 | 15 | 15 | 15 | 16 | 16 | 17 | 17 | 17 | 18 |
| **Section** | 1 | CC | 3 | CC | 1 | CC | CC | 2 | 3 | CC | 1 | 3 | CC | 3 | CC | 2 | 5 | CC | |
| Coccolithus cf. pelagicus[a] | F | F | F | F | | R | | | X | F | F | | | F | F | F | | F | |
| Cyclococcolithina macintyrei | R | F | R | R | | X | | X | | R | R | | X | R | R | R | | | |
| Discoaster variabilis group[b] | A | F | A | C | | R | R | | | F | R | | | F | | R | | | |
| Helicopontosphaera kamptneri group | C | F | R | F | | X | | | | F | R | | | F | R | | F | F | |
| Reticulofenestra pseudoumbilica | A | C | A | C | R | R | | R | X | F | C | R | F | C | F | F | F | F | |
| "Scyphosphaera"[c] | | X | | | | | | | | R | | | | R | R | | | | |
| Sphenolithus moriformis group[d] | R | R | R | X | | | | | | R | R | | | F | F | R | | F | |
| Triquetrorhabdulus rugosus | | X | X | | | | | | | X | | | X | X | | X | | | |
| Discolithina (many pores) | | X | | X | | | | | | | | | | R | | | X | R | |
| Reticulofenestra n. sp. A | R | R | F | F | | | | | | | | | R | C | F | | R | R | |
| Cyclococcolithina rotula | | R | R | X | | | | | | | X | | | R | | R | R | X | |
| Catinaster calyculus | R | | | | | | | | | | | | | | | | | | |
| Catinaster coalitus | C | F | C | | | | | | | | | | | | | | | | |
| Coccolithus eopelagicus | | | | | | | | | | | | | | R | R | | | R | |
| Discoaster deflandrei | X | | | | | | R | X | | | | | | X | | R | | | |
| Discoaster exilis | | | | | | | R | R | R | F | C | F | C | A | C | C | C | C | |
| Cyclicargolithus floridanus | | | | | | | | | | | F | R | | A | F | C | F | F | |
| Sphenolithus heteromorphus | X | | | | | | | | | | | | | R | | X | | R | |
| Discolithina (imperforate) | | | | | | | | | | | | | | | | X | | | |
| Helicopontosphaera euphratis | | | | | | | | | | | | | | | | R | | | |
| Discoaster divaricatus | | | | | | | | | | | | | | | | | R | | |
| **OVERALL FREQUENCY** | A | C | A | C | R | R | R | R | R | F | C | F | C | A | C | C | C | C | |
| **COCCOLITH PRESERVATION** | M | M | M | P | P | P | P | P | P | M | P | P | P | M | P | P | P | P | |

Note: See footnotes, Table 5.

2/2 part of the *Sphenolithus ciperoensis* (NP25) Zone of Martini (1971). In all probability these samples are also correlatives of the early Waitakian part of the *Discoaster deflandrei* Zone of Edwards (1971).

The remaining Core 24 samples examined, namely those from Section 2 at 84 cm through to the core catcher interval, were collected exclusively from the nannofossil ooze beds and contain abundant low-diversity poorly to moderately well preserved residual assemblages. In underlying samples containing *S. belemnos* and overlying, except for the core catcher, the main range of *S. ciperoensis,* these floras occupy a position high in the Late Oligocene 2/2 part of the *Sphenolithus ciperoensis* (NP25) Zone of Martini (1971). The occurrence of very rare *S. ciperoensis* in Section 2 at 84 and 94 cm may be due to very minor almost penecontemporaneous reworking.

Cores 25, 26, and 27, from 283 to 310 meters and with 3.8-, 6.4-, and 7.8-meter recoveries, respectively, consist of finely bedded, and often mottled, glass shard bearing nannofossil chalks with occasional thin glass shard, zeolite, iron oxide, vitric tuff, or feldspar-rich horizons. As might be expected from these lithologies, the samples taken yielded abundant, but occasionally common, variably preserved residual assemblages of low to moderately low diversity (Table 8). In several samples, the preservation is excellent, but these are exceptional.

The nannofloras of Core 25, Section 1 through to Core 27, Section 4 are interpreted, on the ground of the consistent presence of the name bearer, as occupying a position low in the Late Oligocene 2/2 part of the *Sphenolithus ciperoensis* (NP25) Zone of Martini (1971). According to Martini (1971, p. 763), this zone occurs in the upper part of the stratotype Bormidian Stage of Italy. A correlation of this interval with the Duntroonian Stage of New Zealand (see Edwards, 1971) also seems possible judging from the occurrence of *Chiasmolithus oamaruensis* (mostly without central structure) and *Zygrhablithus bijugatus* in the core catchers of Cores 25 and 16. However, such a correlation, although probably correct, is made uncertain by the associated occurrence of a single specimen

**TABLE 7**
**Distribution of Calcareous Nannofossils, Cores 19-24, Site 205**

| | 1 | 2 | 3 | 4 | 5 | 6 | 7 | 8 | 9 | 10 | 11 | 12 | 13 | 14 | 15 | 16 | 17 | 18 |
|---|---|---|---|---|---|---|---|---|---|---|---|---|---|---|---|---|---|---|
| Adopted Age | Mid Miocene | | | | | | | | Late Oligocene | | | | | | | | | |
| Adopted Zone | ~NN5 | | | | | | | | NP25 (lower) | | | | | | | | | |
| Lithologic Unit | Glass shard ash and minor nannofossil ooze | | | | | | | | Glass shard bearing nannofossil ooze and chalk interbedded with nannofossil vitric ash | | | | | | | | | |
| Depth Below Sea Floor (m) | 169-178 | 178-187 | 198-207 | 216-225 | 246-255 | | | | 274-283 | | | | | | | | | |
| Core | 19 | 20 | 21 | 22 | 23 | | | | 24 | | | | | | | | | |
| Section | CC | 2 | CC | CC | CC | 2 | 4 | CC | 2 | 2 | 2 | 2 | 2 | 2 | 3 | 3 | 4 | CC |
| Depth in section (cm) | | 25 | | | | 27 | 5 | top | 22 | 45 | 53 | 84 | 94 | 130 | 65 | 110 | 86 | base |
| *Coccolithus* cf. *pelagicus*[a] | R | R | F | | R | | | | R | F | F | R | F | R | F | F | R | F |
| *Cyclococcolithina macintyrei* | X | R | R | | R | | | | | | | | | | | | | |
| *Helicopontosphaera kamptneri* group | R | F | F | | F | | | | | | | | | | | | | |
| *Reticulofenestra pseudoumbilica* | F | C | C | | F | | X | F | F | | | | | | | | | |
| *Sphenolithus moriformis* group[b] | R | R | F | X | R | | | R | R | F | F | C | C | A | A | C | | C |
| *Discolithina* (many pores) | | X | F | | | | | | | | | | | | | | | |
| *Cyclococcolithina rotula* | X | R | | | | | | | | | | | | | | | | |
| *Coccolithus eopelagicus* | | R | | | | | | R | R | R | | R | R | R | R | X | | |
| *Discoaster deflandrei* | | | | | | X | X | C | R | A | C | A | C | A | A | C | C | C |
| *Discoaster exilis* | | C | | | | F | R | C | F | R | R | R | | | | | | |
| *Cyclicargolithus floridanus* | R | A | F | R | F | | C | A | C | A | A | A | D | C | D | D | R | C |
| *Discolithina* (imperforate) | X | | R | | X | | | | | | | | | | | | | |
| *Helicopontosphaera euphratus* | | R | X | | | | | | | | | | | | | | | |
| *Discoaster divaricatus* group | F | F | C | F | R | | | R | R | R | | | | | | | | |
| *Holodiscolithus solidus* | | | R | | | | | | | | | | | | | | | |
| *Reticulofenestra bisecta* | | | | | | | | | F | F | F | C | C | C | A | | R | A |
| *Sphenolithus belemnos* | | | | | | | | | F | R | | | | | | | | |
| *Sphenolithus capricornutus*[c] | | | | | | | | | R | X | | | | | | | | |
| *Triquetrorhabdulus carinatus* | | r | | r | | | | | R | R | F | R | R | R | A | C | R | R |
| *Coronocyclus serratus* | | | | | | | | | | | | R | | | R | R | | R |
| *Sphenolithus ciperoensis* | | | | | | | | | | X | X | | | | | | | R |
| OVERALL FREQUENCY | F | C | C | F | C | R | C | A | C | A | A | A | A | A | A | A | C | A |
| COCCOLITH PRESERVATION | P | M | M | P | M | P | P | M | M | M | P | P | P | P | M | M | P | M |

Note: See Table 3 for explanation of symbols.

[a]See Table 5, footnote 1.

[b]See Table 5, footnote 4.

[c]Branched varient of *S. belemnos?*

of *Discoaster saipanensis* (shipboard identification only despite intensive shore laboratory search) and of a questionable specimen of *Corannulus germanicus*. All four species occur in Late Eocene strata and one, *D. saipanensis*, ranges no higher. But if these taxa are reworked, the absence of the ubiquitous mid-Eocene to Early Oligocene species *Reticulofenestra placomorpha* is anomalous.

The Core 27, Section 6 and core catcher samples yielded assemblages essentially similar to those above but also contain *Sphenolithus distentus* and thus conform to the Oligocene *S. distentus* (NP24) Zone of Martini (1971). Since they lack *S. predistentus* they appear to belong to the upper part of his zone, i.e., the part recognized (Martini, 1971, p. 762) in the lower, Chatt A, part of the Rupelian stratotype of Germany. Accordingly, the writer here considers that part of the NP24 Zone overlying the highest

appearance of *S. predistentus* to be of Late Oligocene 1/2 age.

Cores 28, 29, and 30, from 310 to 337 meters and with 6.9-, 8.3-, and 4.2-meter recoveries respectively, essentially consist of lithified iron oxide rich nannofossil ooze finely interbedded with usually thinner nannofossil-bearing glass shard ash horizons. The nannofossil oozes yielded abundant moderately diverse poor to moderately well preserved residual nannofloras. However, in the lowest part of Core 30, a very stiff nannofossil ooze bed abruptly overlies an apparently sparsely fossiliferous thin hard limestone bed basally intruded by a basalt sill.

The Core 28 and 29 samples, like those immediately overlying, contain assemblages conforming to the Late Oligocene 1/2 part of the *Sphenolithus distentus* (NP24) Zone of Martini (1971). The occurrence of *Sphenolithus*

**TABLE 8**
**Distribution of Calcareous Nannofossils, Cores 25-30, Site 205**

| | Late Oligocene | | | | | | | | | | | | | | | | Mid Oligocene | | |
|---|---|---|---|---|---|---|---|---|---|---|---|---|---|---|---|---|---|---|---|
| Adopted Age | | | | | | | | | | | | | | | | | | | |
| Adopted Zone | NP25 (lower) | | | | | | NP24 (upper) | | | | | | | | | | NP24 (lower) | | n.d |
| Lithologic Unit | Glass shard bearing nannofossil ooze and chalk interbedded with nannofossil vitric ash | | | | | | | | | | | | | | | | | | |
| Depth Below Sea Floor (m) | 283-292 | | | 292-301 | | | 301-310 | | | 310-319 | | | 319-328 | | | | 328-337 | | |
| Core | 25 | | | 26 | | | 27 | | | 28 | | | 29 | | | | 30 | | |
| Section | 1 | 3 | CC | 2 | 4 | CC | 4 | 6 | CC | 2 | 4 | CC | 2 | 4 | 5 | CC | 1 | 3 | CC |
| Depth in Section (cm) | 147 | 25 | | 25 | 87 | | 35 | 80 | | 25 | 25 | | 25 | 30 | 145 | | 140 | 125 | |
| *Coccolithus* cf. *pelagicus*[a] | F | F | F | R | F | F | C | R | R | F | C | F | C | F | F | F | F | | |
| *Sphenolithus moriformis* group[b] | F | F | C | R | R | C | C | F | F | C | C | C | C | C | C | C | C | C | |
| *Coccolithus eopelagicus* | | R | R | R | R | R | R | F | F | F | R | R | R | R | R | R | R | C | |
| *Discoaster deflandrei* | A | A | C | R | F | A | A | F | C | F | C | | C | R | R | F | F | F | |
| *Cyclicargolithus floridanus* | C | C | A | C | A | D | D | A | A | A | A | D | A | D | D | A | A | A | R |
| *Reticulofenestra bisecta* | D | D | A | F | A | R | | | R | C | C | A | A | A | A | A | C | D | |
| *Triquetrorhabdulus carinatus* | R | R | R | F | F | | | | R | | | R | R | R | R | R | X | X | |
| *Coronocyclus serratus* | | | R | | | | F | | | | | | | | | | | | |
| *Sphenolithus ciperoensis* | R | R | F | | R | | R | R | R | R | R | F | F | F | F | R | R | R | |
| *Chiasmolithus oamaruensis* | | | X | | | | | | | X | | | X | | X | | | | |
| *Zygrhablithus bijugatus* | | | | | | R | | | | | | | | X | X | | | | |
| *Sphenolithus distentus* | | | | | | | | | | R | R | R | F | F | F | F | F | R | |
| *Discoaster tani nodifer?* | | | | | | | | | | | | X | | R | R | | R | R | |
| *Sphenolithus pseudoradians* | | | | | | | | | | | | | | R | R | X | R | R | |
| *Sphenolithus predistentus* | | | | | | | | | | | | | | | | | R | R | |
| *Discoaster saipanensis* | | | x | | | | | | | | | | | | | | | | |
| *Corannulus germanicus?* | | | | | | x | | | | | | | | | | | | | |
| *Reticulofenestra placomorpha* | | | | | | | | | | | | | | | | | | r | |
| OVERALL FREQUENCY | A | A | A | C | A | A | A | A | C | A | A | A | A | A | A | A | A | A | R |
| COCCOLITH PRESERVATION | M | M | G | P | G | G | M | M | M | M | M | P | M | M | P | P | P | M | P |

Note: See Table 3 for explanation of symbols.

[a]See Table 5, footnote 1.

[b]See Table 5, footnote 4.

*pseudoradians* in the lower part of Core 29 is particularly interesting because neither Martini (1971) nor Roth et al. (1971) have recorded this very distinctive species above the lowest appearance of *Sphenolithus ciperoensis,* i.e., the base of the NP24 Zone. However, the consistent presence in both cores of *Triquetrorhabdulus carinatus* supports (see Roth et al. 1971, figs. 1, 4) the writer's conclusion that *S. ciperoensis* is present to the base of Core 29 and below.

The Core 30, Section 1 and Section 3 samples, in containing *Sphenolithus ciperoensis, S. distentus,* and *S. predistentus* plus *T. carinatus,* conform to the mid Oligocene 2/2 part (as defined above) of the *Sphenolithus distentus* (NP24) Zone of Martini (1971). The lowest sample, just a few centimeters above the top of the limestone, also contains rare battered *Reticulofenestra placomorpha.* The presence of this species is significant because it implies minor reworking from mid Eocene to Early Oligocene strata. In view of the apparent presence of very rare reworking from strata no younger than Late Eocene in the overlying Cores 25 and 26, a mid or Late Eocene source seems probable.

The Core 30 core catcher sample appears to consist largely of small granules of calcite. Since this sample is immediately underlain by a basalt sill, the calcite is considered to be authigenic and to have resulted from the recrystallization of nannofossil ooze. The rare calcareous nannofossils observed under the light microscope all appear to belong to *Cyclicargolithus floridanus,* a species known to range from the Late Eocene into the mid Miocene.

Cores 31 and 32 were not examined for calcareous nannofossils as they mostly consist of basalt, and the only sedimentary strata present (in Core 31 Section 1) is a thin hard limestone similar to that of the immediately overlying Core 30 core catcher.

All of the assemblages discussed above appear to have originated from warm subtropical oceanic near-surface waters which probably formed part of a South Pacific subtropical anticyclonic gyral similar to that existing today

(Knox, 1970). Likewise, deposition throughout the sequence recovered appears to have been at abyssal depths not greatly different from that occupied today despite the present day accumulation of sediments lacking nanno-fossils. These conclusions are based on the relative ease with which this sequence can be correlated with the zonal scheme of Martini (1971), the virtual absence (but see below) of taxa preferring neritic environments, the residual nature (i.e., high nannolith to coccolith ratio) of the assemblages, and the known complex undulations of the calcium carbonate compensation depth (Berger, 1971; Benson et al., 1970). Variations in the sill depth of the South Fiji Basin and in the depositional factors discussed below probably had significant regional and local effects on the calcium carbonate compensation depth.

Deposition rates, uncorrected for compaction, as calculated from the calcareous biostratigraphy and matched to the time scale by Bukry (1971) are as follows:

| Interval | Deposition rate (m/m.y.) | Dominant sediment |
|---|---|---|
| Plio-Pleistocene | ~2 | Abyssal clay |
| Late Miocene | 10 | Nannofossil ooze |
| Mid Miocene | 55 | Tuffaceous sandstone |
| Early Miocene | — | No record. |
| Oligocene | ~10 | Nannofossil ooze |

That the mid-Miocene and Early Pliocene sediments have been deposited after bottom current transport can be deduced from the small battered assemblages, sometimes containing the neritic genus *Discolithina*, characteristic of the mid Miocene, and from the prominent reworking evident in the Early Pliocene flora. The source of the mid Miocene sediments was probably close to the summit of the Lau Ridge whereas the Early Pliocene source was almost certainly the nearby ridge at the present foot of the Lau Ridge sediment apron. These conclusions, coupled with the deposition rates given above and the accompanying lithologic changes, strongly suggest that the nearby ridge, mentioned above, was formed or accentuated during the Late Miocene. The basalt sill at the base of the Site 205 sequence may well be of similar age. Simple extrapolation of the Oligocene deposition rate down to the acoustic basement, although speculative, suggests an age of about Early Eocene for the latter.

## Synopsis

At Site 205, near the eastern margin, of the South Fiji Basin residual calcareous nannofossil assemblages indicative of warm subtropical oceanic conditions were deposited, together with greatly varying amounts of tuffaceous debris, at abyssal depths during late mid Oligocene to Early Pliocene time. Deposition at this site may have commenced during the early Paleogene. The Early Miocene is not represented. During the Late Miocene, uplift on a nearby ridge probably caused the deposition pattern to gradually change towards that existing today.

## SOME COMMENTS ON THE BIOSTRATIGRAPHY

There can be little doubt that statements about southwest Pacific biostratigraphy which are relatable to the New Zealand Cenozoic Stage classification (Table 9) have far more value than those which are expressed in terms of the equivalent International classification of epochs and their subdivisions. This is so because the former is nearby and is based on more or less continuous sequences deposited under offshore conditions, whereas, the latter is essentially based on discontinuous shallow-water deposits in Europe, some 20,000 kilometers distant. There are, of course, notable exceptions to the above generalization; for example, neither scheme is very satisfactory in the Paleocene. The following comments provide information on the major relationships of these two classifications over and above those provided by Edwards (1971).

### The Oligocene-Miocene Boundary

This boundary is generally placed at the base of the Aquitanian Stage of France, which unfortunately lacks calcareous nannofossils at it's stratotype (Bramlette & Wilcoxon, 1967, p. 100; Edwards, 1971, p. 415). This being the case, the next best approximation to this boundary would be the top of the underlying Chattian Stage of Germany. Unfortunately, the neostratotype of this stage was deposited under very shallow-water conditions and only sparse, long ranging calcareous nannofossils are present (Anderson et al., 1971; Haq, 1971). These include *Reticulofenestra bisecta* (= *R. scissura;* recorded in

**TABLE 9**
**The Late Cretaceous and Cenozoic Stage Classification of New Zealand and Their Approximate International Correlatives**

| International | | New Zealand | |
|---|---|---|---|
| Epoch | | Stage | Symbol |
| Pleistocene | | Hawera (Series) | Q |
| | | Castlecliffian | Wc |
| | | Nukumaruan | Wn |
| Pliocene | | Waitotaran | Ww |
| | | Opoitian | Wo |
| | | Kapitean | Tk |
| Miocene | late | Tongaporutuan | Tt |
| | mid | Waiauan | Sw |
| | | Lillburnian | Sl |
| | | Clifdenian | Sc |
| | early | Altonian | Pl |
| | | Otaian | Po |
| | | Waitakian | Lw |
| Oligocene | | Duntroonian | Ld |
| | | Whaingaroan | Lwh |
| Eocene | late | Runangan | Ar |
| | | Kaiatan | Ak |
| | mid | Bortonian | Ab |
| | | Porangan | Dp |
| | | Heretaungan | Dh |
| | early | Mangaorapan | Dm |
| | | Waipawan | Dw |
| Paleocene | | Teurian | Dt |
| Late Cretaceous | | Haumurian | Mh |
| | | Piripauan | Mp |
| | | Teratan | Rt |
| | | Mangaotanean | Rm |
| | | Arowhanan | Ra |
| | | Ngaterian (= Coverian) | Cn |
| | | Motuan | Cm |

Anderson et al., 1971 as "*Dictyococcites dictyodus*") and *Zygrhablithus bijugatus*, both of which are consistently present and have their highest occurrences just five meters below the top of the neostratotype. That these occurrences are within the upper parts of the ranges of these taxa is suggested by the presence of very sporadic "*Coccolithus*" *abisectus* and objects resembling *Triquetrorhabdulus carinatus*. Both taxa are characteristic of Late Oligocene and Early Miocene strata elsewhere. All of these taxa could be present because of reworking, but this seems unlikely since correlations using the extinctions of *R. bisecta* and (slightly younger) *Z. bijugatus* provide results which appear to be consistent with those deduced from the planktonic foraminifera (compare Scott, 1972 with the biostratigraphic summaries given for Sites 206, 208, and 209).

Studies of southwest Pacific material have clearly demonstrated that the extinction of the solution prone and climatically restricted (subtropical) *Z. bijugatus* occurs subsequent to that of *R. bisecta* and prior to that of the much more sporadic *Helicopontosphaera recta*, which Martini (1971) selected as the boundary marker. The writer therefore suggests that the best approximation to the Oligocene-Miocene boundary using the calcareous nannofossils is the extinction level of the abundant, distinctive, highly solution resistant, and ubiquitous *Reticulofenestra bisecta* (Hay, Mohler and Wade) Roth (=*R. scissura* Hay, Mohler & Wade). In New Zealand, this datum level occurs within the early Waitakian Stage (Edwards, 1971).

## The Mesozoic-Cenozoic Boundary

The recovery of a near complete sequence across the Maastrichtian-Danian boundary at Site 208 in the northern Tasman Sea is of exceptionally high scientific interest. This is largely due to its relevance to modern hypotheses on the origin of the world-wide unconformity associated with this boundary in marine sequences (see discussion in Chapter 20). However, this record of the boundary also has high regional significance because it provides the first southwest Pacific sequence in which this feature can be pinpointed using positive biostratigraphic data. Elsewhere in the southwest Pacific, the Maastrichtian-Danian boundary is placed at the top of the interval containing Cretaceous taxa; that is, at the boundary between the Haumurian (late Cretaceous) and Teurian (Paleocene) stages of New Zealand (Hornibrook, 1962). There is little doubt that this boundary has been correctly placed, but the immediately overlying strata either contain taxa indicative of the presence of a substantial disconformity or, at other more continuous localities, lack calcareous microfossils useful for correlation with the early Danian type area (Edwards, 1971, p. 386; Hornibrook, 1972, p. 181; Ludbrook, 1967, p. 9).

The calcareous nannofossil assemblages obtained from the immediate vicinity of the Mesozoic-Cenozoic boundary in Site 208 are given in Table 10. There is clearly a very close coincidence between the lithostratigraphic and biostratigraphic units. This correspondence is especially obvious when the lithologic boundaries are adjusted for probable burrowing activity and sediment inversion during or subsequent to drilling (see discussion in Chapter 20). Unity is reached when minor downhole contamination and

significant uphole reworking is taken into account. Such a situation, plus the obviously slow overall deposition rate (see Chapter 20), clearly implies that the Site 208 sequence is incomplete due to the loss, or nondeposition, of sediment at several horizons. However, correlations based on nannofossils clearly indicate the presence of a sequence which is more complete across the Mesozoic-Cenozoic (Maestrichtian-Danian) boundary than across the same boundary in the Teurian stratotype (Edwards, 1971, p. 386; Hornibrook, 1972, p. 181) and Maastrichtian type area (Vangerow & Schloemer, 1967) sequences. In addition, there is a distinct possibility (see below) that the Site 208 sequence is more complete across this boundary than that at the early Danian stratotype. However, if the Danian stratotypes were superimposed on the Maastrichtian type area, the resultant sequence would be as complete as, and certainly far less condensed than, the Site 208 sequence. Consequently, there seems no good reason to suppose that the sequence at Site 208 contains sediments not represented elsewhere.

Before discussing the calcareous nannofossil biostratigraphy of the Mesozoic-Cenozoic boundary, it is necessary to discuss aspects of the underlying Maastrichtian biostratigraphy. For several years, the writer has suspected, largely on the reported cooccurrence of *Nephrolithus barbarae* (= *N. frequens*) and *Lucianorhabdus cayeuxi* in the "lower" Maastrichtian Kjolby Gard (Denmark) sample 6 of Bramlette & Martini (1964), that these two species (or genera) overlapped in what might be loosely called mid Maastrichtian. At Site 208, such a concurrent range occurs for at least 11 meters, and accordingly, for Leg 21 purposes, an informal subdivision of the *Nephrolithus frequens* Zone into two parts was adopted (Chapter 2). Such a subdivision is compatible with the nannofossil data provided by Bramlette & Martini (1964), Vangerow & Schloemer (1967), Perch-Neilsen (1969), Edwards (1971), and many others for widely separated Maastrichtian localities which include Denmark, Holland, Tunisia, and New Zealand. Although Cepek & Hay (1969) did not record an overlap of *N. frequens* and *L. cayeuxi* in Alabama, this is probably due to the known provinciality of *N. frequens* (Worsley & Martini, 1970) rather than to a diachronous last appearance of *L. cayeuxi*.

In order to better understand the Site 208 succession, the writer examined the comparable sequence across the Mesozoic-Cenozoic boundary at Hojerup, Stevns Klint, Denmark; that is, the Stevnsian ("upper" Maastrichtian) and basal Danian in their type areas (Table 11). Surprisingly, both *N. frequens* and *L. cayeuxi* were recorded throughout the Stevnsian, a situation contrary to the results of both Bramlette & Martini (1964) and Perch-Neilsen (1969). The reason for these contradictory results is not known but, apart from several specimens of *Watznaueria barnesae*, no obviously reworked taxa were noted. Furthermore, neither Bramlette & Martini (1964) nor Vangerow & Schloemer (1967) recorded *L. cayeuxi* from the type area Maastricht Chalk of Holland although the latter paper lists this taxon as persistently present in the immediately underlying Gulpen Chalk. Thus, correlations based on the last appearance of *L. cayeuxi* imply that the uppermost part of the White Chalk (Stevnsian; "upper"

**TABLE 10**
Calcareous Nannofossil Occurrence and Biostratigraphy across the Mesozoic – Cenozoic
Boundary Sequence Recovered in DSDP Site 208, Core 33, Section 1

Column groups (left to right): Age (Stage) [Adopted / Indicated]; Biostratigraphic Zones [Inferred / Observed]; Lithostratigraphic Units (informal) [Inferred / Observed]; Photographic Scale (cm.); Core 21-208-33-1 (17 to 101 cm); Calcareous Nannofossil Samples (cm.); Calcareous Nannofossil Frequency; then species occurrence columns under the headings **Mesozic Species**, **?M**, **M–C**, and **Cenozoic**, and a final column **Obvious contamination from uphole sediments**.

Stratigraphic framework (top to bottom):

| Age (Stage) | Biostratigraphic Zone | Lithostratigraphic Unit |
|---|---|---|
| early Danian | Cruciplacolithus tenuis | D (silicitite) |
| basal Danian | Conococcolithus panis | C (silicitite) |
| late Maastrichtian | Nephrolithus frequens (upper part) | B (silicitite) |
| mid Maastrichtian | Nephrolithus frequens (lower part) | A (chalk) |

Note within samples column (near 80–82 cm): "upward loss due to increased diagenesis?"

Photographic scale marks: 20, 30, 40, 50, 60, 70, 80, 90, 100 cm. Sample depths (cm) with nannofossil frequency: 20 (V), 23 (V), 30 (V), 36 (V), 45 (V), 54 (V), 58 (V), 60 (R), 74 (V), (81), 82 (F), 95 (A).

Species occurrence matrix (species as rows, sample depth in cm as columns):

| Species | 20 | 23 | 30 | 36 | 45 | 54 | 58 | 60 | 74 | 82 | 95 |
|---|---|---|---|---|---|---|---|---|---|---|---|
| Ahmuellerella octoradiata (Gorka) | | | | | | | | | X | V | R |
| Cribrosphaerella ehrenbergii (Arkhangelskii) | | | | | | | | | | X | X |
| Eiffellithus eximus (Stover) | | | | | | | | | | X | X |
| Eiffellithus turriseiffeli (Deflandre) | | | | | | | | | | X | R |
| Kamptnerius magnificus Deflandre | | | | | | | | | | | V |
| Lucianorhabdus cayeuxi Deflandre | | | | | | | | | | | X |
| Microrhabdulus decoratus Deflandre | | | | | | | | | | | F |
| Chiastozygus amphipons (Bramlette & Martini) | x | | x | | | x | X | | X | X | X |
| Cretarhabdulus surriellus (Deflandre & Fert) | | | x | | | x | X | | X | X | V |
| Deflandrius cretaceus (Arkhangelskii) | | | | | | x | X | | X | | R |
| Deflandrius spinosus Bramlette & Martini | | | | | | x | X | X | X | R | C |
| Nephrolithus frequens Gorka | | | | | | | X | X | X | X | R |
| Zygodiscus spiralis Bramlette & Martini | | | | | | x | V | X | V | R | F |
| Arkhangelskiella cymbiformis Vekshina | v | x | x | | | x | V | X | V | R | R |
| Micula staurophora (Gardet) [?M] | x | x | r | v | | f | F | R | V | R | R |
| Crepidolithus sp. [M–C] | | | | | | X | | | | | |
| Markalius astroporus (Stradner) [M–C] | X | V | X | | | V | V | X | | | |
| Thoracosphaera operculata Bramlette & Martini [Cenozoic] | X | | | | | X | | | | | |
| Biantholithus sparsus Bramlette & Martini | | | | X | | V | | | | | |
| Conococcolithus panis Edwards | X | X | X | X | | X | x | | | | x |
| Zygodiscus sigmoides Bramlette & Sullivan | V | X | R | V | X | X | | | | | |
| Cruciplacolithus tenuis (Stradner) | V | X | V | | | X | | | | | |
| Hornibrookina teuriensis Edwards | | | | x | | | | | | | |
| Obvious contamination from uphole sediments | x | | | v | | | v | x | | | r |

Note: See Table 3 for an explanation of symbols.

655

Maastrichtian) of Denmark is older than the Maastricht Chalk (type "upper" Maastrichtian) of Holland. Such a hypothesis is contrary to both traditional and modern correlations between these two sequences (Berggren, 1964). These latter correlations are apparently based on similar sequential positions plus the occurrence of *Belemnella casimirovensis* in both sequences. Unfortunately, the belemnite correlation, apparently, is based entirely on one small fragment of *B. casimirovensis* in the Maastricht Chalk (Birkelund, 1957, p. 65). The calcareous nannofossil based hypothesis (Table 12) that the uppermost White Chalk and the Maastricht Chalk are not correlatives is thus quite feasible and certainly well worth further investigation by biostratigraphers. One question that clearly needs answering is whether the absence of *L. cayeuxi* in the Maastricht Chalk is due to ecologic exclusion—the distribution of this species suggests that it prefers warm oceanic waters—or to its prior extinction.

Reworking is conspicuous just above the Mesozoic-Cenozoic boundary at Site 208 (Table 10), Stevns Klint (Table 11) and other Danish localities (Perch-Nielsen, 1969, table 1), Curfs, near Houthem, Holland (Vangerow & Schloemer, 1967), and many other localities. Consequently any zonal boundary intended to coincide with the major floral change at the Mesozoic-Cenozoic boundary must, for practical reasons, be based on the first appearance of a Danian taxon. To date, no such workable definition has been proposed largely because of the rarity of the only highly distinctive Danian species, *Biantholithus sparsus*. The writer believes that the base of the variable, but moderately distinctive and common, *Conococcolithus panis* provides the best definition presently available for the Mesozoic-Cenozoic boundary. Accordingly, the following new basal Danian zone is formally proposed using the same procedures as given in Edwards (1971):

### *Conococcolithus panis* Zone

Definition: Interval between the lowest appearance of *Conococcolithus panis* Edwards and the lowest appearance of *Cruciplacolithus tenuis* (Stradner) Hay & Mohler.

Accompanying distinctive taxa: Lowest known occurrence of *Biantholithus sparsus* Bramlette & Martini and *Zygodiscus sigmoides* Bramlette & Sullivan. Also, often present are *Braarudosphaera bigelowi* (Gran & Braarud) Deflandre, *Crepidolithus* Noel, *Markalius astroporus* (Stradner) Hay & Mohler, and *Thoracosphaera operculata* Bramlette & Martini.

Distribution: From the base of the Fish Clay to the lowest part (base plus 0.6 meters) of the Bryozoan Limestone interval in the Stevns Klint at Hojerup section, Denmark (Table 11). Also, between 30 and 57 cm (informal lithostratigraphic unit C) in Core 33, Section 1 of Site 208 on the northern Lord Howe Rise, Tasman Sea (Table 10). Unit C is at present at a subbottom depth of 576 meters below a 1555 meter water column at 26°06.61'S, 161°13.27'E.

Adopted age: Earliest Danian (basal Teurian?).

Correlations: See Table 12.

Remarks: The presence of extremely rare specimens of *C. panis* in the underlying *Nephrolithus frequens* Zone of both sequences is attributed to very minor downward contamination. The evidence for such a conclusion is strong at Site 208 (see Table 10) and plausible at Stevns Klint which is a near vertical cliff. Furthermore, the complete absence of *C. panis* in all of the New Zealand *N. frequens* Zone nannofloras examined by the writer supports such a conclusion. In the southwest Pacific, *C. panis* has a short biostratigraphic range entirely within Danian equivalents.

The reworking present in the *C. panis* Zone at Site 208 probably came from the underlying chalk, the "mid" Maastrichtian top of which underlies this zone by only 22 cm (Table 10). In marked contrast, only a minor amount of the initially copious reworking present in this zone at Stevns Klint appears to have come from the uppermost part of the underlying White Chalk. The majority of the reworking appears to have come from older late Cretaceous strata since this reworking consistently includes a species, *Watznaueria barnesae*, almost completely absent from the immediately underlying chalk (Table 11).

It is customary to consider almost all of the Mesozoic species found in Cenozoic sediments as resulting from reworking. Undoubtedly, this is true of most taxa, but two species stand out due to their greater frequency and consistency of occurrence. These are *Arkhangelskiella cymbiformis* and, especially, *Micula staurophora*. These forms are probably more resistant to solution and fragmentation than other Mesozoic species. However, it is just conceivable that these species, like *Crepidolithus*, survived into the basal part of the Danian.

All attempts by the writer to obtain electron micrographs of *C. panis* have so far failed. However, a possible transmission electron micrograph of *C. panis* was figured by Hoffmann (1972, Pl. 10, fig. 4), as a proximal view of *Biscutum constans* (Gorka) Black, from the *Tylocidaris abildgaardi* Zone (early Danian) of Boesdal, Denmark.

## THE POTENTIAL FOR CLIMATIC BELT ZONATIONS

The Cenozoic calcareous nannofossil assemblages obtained from the Coral Sea and Fiji Sea sites have numerous taxa in common with the equivalent nannofloras obtained from the Tasman Sea sites and New Zealand. However, while the differences between these two areas are relatively minor in the Eocene, this certainly is not true of the Oligocene to Pleistocene interval during which the possibilities for accurate inter-regional correlation are not great (see Chapter 2).

This situation, which in effect reflects the known climatic provincialism of many calcareous nannofossils, is attributed to the complex interaction of three distinct factors. These are: (a) the slow northward (equatorward) movement of the southwest Pacific during the Cenozoic in response to sea floor spreading south of Australasia (Le Pichon & Heirtzler, 1968; Wellman et al., 1969), (b) the overall southward (polewards) movement, at least during the Neogene, of near-surface waters having a circulation

## TABLE 11
### Calcareous Nannofossil Occurrence and Biostratigraphy across the Mesozoic – Cenozoic Boundary Sequence Exposed at Hojerup, Stevns Klint, Denmark

| Age (Stage) | Biostratigraphic Zones | Column and Lithostratigraphic Units (after Rasmussen, 1971) | Calcareous Nannofossil Samples (N.Z. Geological Survey catalogue numbers) | Cal. Nanno. Freq./Pres. | Mesozoic Species |||||||||||||||| ?M | M–C ||| C ||
|---|---|---|---|---|---|---|---|---|---|---|---|---|---|---|---|---|---|---|---|---|---|---|---|---|---|---|
| | | | | | *Ahmuellerella octoradiata* (Gorka) | *Chiastozygus amphipons* (Bramlette & Martini) | *Cretarhabdulus surriellus* (Deflandre & Fert) | *Cribrosphaerella ehrenbergii* (Arkhangelskii) | *Deflandrius cretaceus* (Arkhangelskii) | *Deflandrius spinosus* Bramlette & Martini | *Eiffelithus turriseiffeli* (Deflandre) | *Kamptnerius magnificus* Deflandre | *Lithraphidites quadratus* Bramlette & Martini | *Lucianorhabdus cayeuxi* Deflandre | *Microrhabdulus decoratus* Deflandre | *Nephrolithus frequens* Gorka | *Watznaueria barnesae* (Black) | *Zygodiscus spiralis* Bramlette & Martini | *Arkhangelskiella cymbiformis* Vekshina | *Micula staurophora* (Gardet) | *Braarudosphaera bigelowi* (Gran & Braarud) | *Crepidolithus* spp. | *Markalius astroporus* (Stradner) | *Thoracosphaera operculata* Bramlette & Martini | *Biantholithus sparsus* Bramlette & Martini | *Conococcolithus panis* Edwards |
| basal Danian | *Conococcolithus panis* | Bryozoan Limestone | N1078 | F/M | x | | x | x | x | | x | | | | | x | v | x | v | x | V | F | F | V | X | F |
| | | local erosion | N1191 | F/M | x | x | | x | x | x | v | x | x | | | x | v | x | f | r | | | F | V | V | R |
| | | Cerithium Lst. (up to 0.8m thick) | N1190/A | A/M | | | x | x | | v | | | v | | x | v | v | v | a | a | | X | R | X | X | F |
| | | Fish Clay (up to 0.2m) | N1190/B | A/M | | | x | | x | | | | | | x | x | x | | c | c | | X | X | | X | X |
| Maastrichtian (mid?) Stevnsian Substage | *Nephrolithus frequens* (lower part) | White Chalk rich in bryozoans (ca. 2.5m. thick) | N1508 | C/M | X | V | X | R | V | | V | V | X | R | V | V | | R | C | R | V | X | | | | x |
| | | White Chalk | N1077 | C/M | X | X | X | V | F | C | X | X | V | F | R | R | x | X | F | R | | | | | | |

Note: See Table 3 for explanation of symbols.

**TABLE 12**
A Speculative Correlation of the Site 208 Sequence with Those Containing the Danian,
Maastrichtian, Stevnsian and Teurian Stratotypes

| Calcareous Nannofossil Biostratigraphic Zones | Northern Europe | | | | South West Pacific | | | | | |
|---|---|---|---|---|---|---|---|---|---|---|
| | Stevns Klint, Denmark (after Table 11 & Rasmussen, 1970) | Age | Maastricht District, Holland (after Vangerow & Schloemer, 1967) | Age | Site 208, Northern Lord Howe Rise (after Table 10) | Age | Te Uri Stream, New Zealand (after Edwards, 1971) | Age | Mid Waipara, New Zealand (after Edwards, 1971) | Age |
| *Chiasmolithus danicus* | Bryozoan Limestone (part) | Danian (part) | Geulem Chalk | Danian | Core 31, Section 3 (75 cm) to Core 32-CC — Contact not observed | Danian | "upper" Whangai | Teurian (part) | Birch Formation | Teurian (part) |
| *Cruciplacolithus tenuis* | | | disconformity | | Informal (Unit D (Silicitite)) — disconformity | | disconformity | | no calcareous nannofossils | |
| *Conococcolithus panis* | disconformity — Cerithium Limestone — Fish Clay | | | | Informal Unit C (Silicitite) | | | | | |
| *Nephrolithus frequens* (upper part) | paraconformity | Stevnsian | hard ground — Maastricht Chalk | Maastrichtian (part) | paraconformity — Informal Unit B (Silicitite) | Magstrichtian (part) | Whangai Formation (part) | Haumurian (part) | ? disconformities — Laidmore | Haumurian (part) |
| *Nephrolithus frequens* (lower part) | White Chalk rich in bryozoans — disconformity — White Chalk (part) | | disconformity — Gulpen Chalk (part) | | disconformity? — Informal Unit A (Chalk) | | no nannofossils | | Formation (part) — no nannofossils | |

pattern similar to that of the present (Knox, 1970), and (c) the more or less gradual growth through the Cenozoic of the present day circum-polar current as a result of events induced by sea floor spreading. The latter development is considered not only to have brought about an increase in the volume of water held at high latitudes but also a corresponding increase in the disparity between the equatorial and subpolar near surface water temperatures. In the writer's opinion, the greatest increase in the temperature disparity occurred across the Eocene-Oligocene boundary and resulted both in the first Cenozoic high latitude refrigeration and, due to the consequent intensification of circulation, in the Eocene-Oligocene regional unconformity (see Chapter 20). Whatever, the interaction of the above and similar factors elsewhere must have caused world-wide sympathetic, but not necessarily corresponding, climatic changes since the world's oceans form a closed system.

The implications for developing a single world-wide high resolution zonal scheme are clear, i.e., that, with several notable exceptions (see below), it is a quite impractical objective. The following four possible alternatives remain: (a) to develop fully an assemblage zonal scheme such as that of Bramlette & Sullivan (1961, p. 134), (b) to greatly increase the geographic distribution of a zonal scheme such as that of Martini (1971) by basing it on more cosmopolitan taxa, (c) to propose different zonal schemes, such as that of Edwards (1971), and local schemes where necessary, or (d) to abandon zonal schemes and use only datum levels.

Application of possibility (a) would result in numerous buffer zones (Hornibrook, 1966); of (b), in a marked decrease especially in the Oligocene and Neogene of the tropics in the degree of biostratigraphic resolution; of (c), in a multiplicity of zonations and thus a complexity of correlations; and of (d), in a simple objective statement of biostratigraphic position providing both great flexibility in the choice of available events and freedom from the necessity of subscribing to a particular zonal scheme.

As is obvious from the above, the writer prefers the fourth possibility. However, since it is current practice to propose zonal schemes some thought should be given to which of the three types of zonations listed above should be given preference. Of these alternatives, the writer prefers the third possibility, for, despite its complexity and the probable variable geographic coverage with time of each climatic belt scheme, it allows maximum biostratigraphic resolution. The writer envisages separate tropical, northern subtropical, southern subtropical, subarctic, and subantarctic schemes. The placolith based cold-water schemes, which probably will not be necessary in the Paleocene and Eocene, should be readily correlatable with the higher resolution subtropical schemes. The latter should, in turn, be correlatable with the tropical schemes via deep-water, warm subtropical sequences rich in nannoliths. Martini's (1971) zonation can be regarded as essentially a tropical scheme, although some modification is needed to take into account those taxa not found south of the equator. This is not to say that parts of his scheme may not be more widely applicable. For example, his late Pleistocene zones, an excellent example of possibility 2 above, can be usefully

recognized as far south as 56°S (Geitzenauer, 1972). However, some diachrony may be involved. To date, only one regional zonation, that of Edwards (1971) for the Paleogene of New Zealand, has been proposed. With some modification, it would provide a useful basis for a southern subtropical zonal scheme.

## PROVINCIALISM IN CALCAREOUS NANNOFOSSILS

In the last few years it has become increasingly apparent that not all calcareous nannofossils have ubiquitous distributions. Many taxa are now known to be characteristic of a particular hemisphere ocean or marginal sea while others are essentially restricted to certain ecologic conditions such as a specific climate or water mass type. Some examples of provincialism noted as a result of Leg 21 studies are given below. It is emphasized that provincialism should not be invoked merely because a taxon is not present in a given facies. Its absence, or loss of identity, may be due to selective dissolution or overgrowth induced by the depth of deposition or diagenesis. Furthermore, consideration should be given to the possibility that a taxon was provincially restricted during only part of its world-wide range.

### Braarudosphaeraceae

This distinctive family is characteristic of warm nearshore areas (Martini, 1961, 1967; Bukry et al., 1971, pp. 1262-1266; and Takayama, 1972) although an apparent notable exception is known in the Oligocene of the South Atlantic (Saito & Percival, in Maxwell et al., 1970, p. 445). In the Leg 21 sequences, the pentaliths of this family were found in significant numbers only in the Early Eocene 3/5 to mid Eocene 1/7 at Site 207 on the southern Lord Howe Rise and the mid Eocene 6/7 to Early Miocene 1/5 at Site 209 on the Queensland Plateau. These two sites were the shallowest and nearest to land, and their paleogeographic histories strongly suggest that these occurrences result from nearby epicontinental conditions which did not persist. Furthermore, pentaliths are extremely rare and stratigraphically very sporadic in the other Leg 21 sequences. This is especially significant in the case of the Site 208 sequence on the northern Lord Howe Rise since this sequence is presently at a depth similar to those at Sites 207 and 209, and it occupies an intermediate geographic position. This pattern leaves little doubt that the braarudosphaerids have a distinct preference for warm epicontinental conditions.

### The Coccolithus pelagicus (Wallich) Stock

As expected, in the Neogene this stock was only common in the southern Leg 21 sequence (especially that at Site 207), but in the Eocene it has a much wider distribution. There seems little doubt that its ecologic preferences have become progressively restricted until today it is characteristic of cool subtropical areas.

### Discoaster barbadiensis Tan Sin Hok

In the southwest Pacific, the highest appearance of this taxon is, as in New Zealand (Edwards, 1971, p. 399), consistently within the mid Eocene 6/7 (Bortonian). Thus,

its range is markedly different from that in the Carribbean, North Atlantic, and Mediterranean areas where its highest appearance is very close to the top of the Late Eocene (Hay *in* Hay et al., 1967, p. 439). The reason for this striking example of provincialism is not known. The writer gained the impression that in the southwest Pacific this species rapidly withdrew to the north, but the biostratigraphic control is not yet adequate to substantiate or deny this supposition.

### Discolithina (including Transversopontis)

Although obviously very closely related to the living genus *Pontosphaera*, this essentially Paleogene group differs in being characteristic of warm nearshore areas (writer's observations, also Bukry et al., 1971, pp. 1262-1266). On Leg 21, this group was found in significant numbers only in the Mid and Late Eocene of Site 209 on the Queensland Plateau and in a single Early Eocene 3/5 sample at Site 207 on the southern Lord Howe Rise. Both these occurrences are within those indicated for the braarudosphaerids above, and thus, by implication, this group has similar ecologic preferences. The only other Leg 21 occurrences noted were in the tuffaceous and were almost certainly largely redeposited, Miocene sediments of Site 205 (see above). Despite its vulnerability to corrosion, the distribution of this group strongly suggests that it had little tolerance to oceanic conditions.

### ACKNOWLEDGMENTS

### REFERENCES

Anderson, A. J., Hinsch, W., Martini, E., Muller, C., and Ritzkowski, S., 1971. Chattian: Gior. Geol., (2), v. 37(2), p. 69-79.

Benson, W. E., Gerard, R. D., and Hay, W. W., 1970. Summary and conclusions: *In* Bader, R. G. et al., Initial Reports of the Deep Sea Drilling Project, Volume IV. Washington (U.S. Government Printing Office), p. 659-673.

Berger, W. H., 1971. Sedimentation of Planktonic Foraminifera: Marine Geol., v. 11(5), p. 325-358.

Berger, W. H. and Heath, G. R., 1968. Vertical mixing in pelagic sediments: J. Marine Res., v. 26(2), p. 134-143.

Berggren, W. A., 1964. The Maestrichtian, Danian and Montian Stages and the Cretaceous-Tertiary Boundary: Stockholm Contr. Geol., v. 11(5), p. 103-176.

Birklund, T., 1957. Upper Cretaceous belemnites from Denmark: Biol. Skr. Dan. Vid. Selsk., v. 9(1), p. 1-69.

Bramlette, M. N. and Martini, E., 1964. The great change in calcareous nannoplankton fossils between the Maestrichtian and Danian: Micropaleontology, v. 10(3), p. 291-322.

Bramlette, M. N. and Sullivan, F. R., 1961. Coccolithophorids and related nannoplankton of the early Tertiary in California: Micropaleontology, v. 7(2), p. 129-188.

Bramlette, M. N. and Wilcoxon, J. A., 1967. Middle Tertiary calcareous nannoplankton of the Cipero Section, Trinidad, W. I.: Tulane Studies Geol., v. 5(3), p. 93-131.

Bukry, D., 1969. Upper Cretaceous coccoliths from Texas and Europe: Kansas Univ. Paleont. Contr. 51 (Protista 2), p. 1-79.

Bukry, D., 1971. Cenozoic calcareous nannofossils from the Pacific Ocean: San Diego Soc. Nat. Hist. Trans., v. 16(14), p. 303-328.

Bukry, D., Douglas, R. G., Kling, S. A., and Krasheninnikov, V., 1971, Planktonic microfossil biostratigraphy of the northwestern Pacific Ocean: Initial Reports of the Deep Sea Drilling Project, Volume VI. Washington (U. S. Government Printing Office), p. 1253-1300.

Cepek, P. and Hay, W. W., 1969. Calcareous nannoplankton and biostratigraphic subdivision of the Upper Cretaceous: Gulf Coast Assoc. Geol. Socs. Trans., v. 19, p. 323-336.

Edwards, A. R., 1971. A calcareous nannoplankton zonation of the New Zealand Paleogene: Plank. Conf., 2nd, Roma 1970, Proc., p. 381-419.

Geitzenauer, K. R., 1972. The Pleistocene calcareous nannoplankton of the subantarctic Pacific Ocean: Deep-Sea Res., v. 19, p. 45-60.

Haq, B., 1971. Paleogene calcareous nannoflora. Part 2, Oligocene of western Germany: Stockholm Contr. Geol., v. 25(2), p. 57-97.

Hay, W. W., Mohler, H. P., Roth, P. H., Schmidt, R. R., and Boudreaux, J. E., 1967. Calcareous nannoplankton zonation of the Cenozoic of the Gulf Coast and Caribbean-Antillean area and transoceanic correlation: Gulf Coast Assoc. Geol. Soc., Trans., v. 17, p. 428-480.

Hayes, D. E. and Ewing, M., 1971. The Louisville Ridge—A possible extension of the Eltanin Fracture Zone: Antarctic Res. Ser. 15 (Antarctic Oceanology 1), p. 223-228.

Hoffman, N., 1972. Coccolithen aus der kreide und dem Palaogen des nordlichen Mitteleuropas: Geologie, v. 21(73), p. 1-121.

Hornibrook, N.de B., 1962. The Cretaceous-Tertiary boundary in New Zealand: New Zealand J. Geol. Geophys., v. 5(2), p. 295-303.

———, 1966. A viewpoint on stages and zones. New Zealand J. Geol. Geophys., v. 8(6), p. 1195-1212.

———, 1972. *Globoconusa daubjergensis* (Foraminifera) at the base of the stratotype of the Teurian Stage, New Zealand: New Zealand J. Geol. Geophys., v. 15(1), p. 178-181.

Jenkins, D. G., 1966. Planktonic Foraminiferal zones and new taxa from the Danian to lower Miocene of New

Zealand: New Zealand J. Geol. Geophys., v. 8(6), p. 1088-1126.

Knox, G. A., 1970. Biological oceanography of the South Pacific. *In* Scientific Exploration of the South Pacific: Washington (National Academy of Sciences), p. 155-182.

Le Pichon, X. and Heirtzler, J. R., 1968. Magnetic anomalies in the Indian Ocean and ocean-floor spreading: J. Geophys. Res., v. 73, p. 2101.

Ludbrook, N. H., 1967. Correlation of Tertiary rocks of the Australasian region. *In* Tertiary Correlations and Climatic Changes in the Pacific: Pacific Sci. Congr., 11, Tokyo, 1966, Symposium 25, p. 7-19.

Manivit, H., 1968. Nannofossiles calcaires du Turonien et du Senonien: Rev. Micropaleont., v. 10(4), p. 277-286.

Martini, E., 1961. Ein kalkflagellat in dem Meeren der Gegenwart und Vorzeit: Natur und Volk., v. 91(9), p. 335-339.

————, 1967. Nannoplankton und Umlagerungserscheinungen im Persischen Gulf und im nordlichen Arabischen Meer: N. Jb. Geol. Paleont. Mh., v. 10, p. 597-607.

————, 1971. Standard Tertiary and Quaternary calcareous nannoplankton zonation: Plank. Conf., 2nd, Roma 1970, Proc., p. 739-785.

Maxwell, A. E., von Herzen, R., et al., 1970. Initial Reports of the Deep Sea Drilling Project, Volume III: Washington (U.S. Government Printing Office), 806 p.

McIntyre, A., 1970. *Gephyrocapsa protohuxleyi* sp. n. a possible phyletic link and index fossil for the Pleistocene: Deep-Sea Res., v. 17, p. 187-190.

McIntyre, A., Be, A. W. H., and Roche, M. B., 1970. Modern Pacific Coccolithophorida: A paleontological Thermometer: New York Acad. Sci. Trans., Series 2, v. 32(6), p. 720-731.

Norris, R. E., 1961. Observations on phytoplankton organisms collected on the N.Z.O.I. Pacific Cruise, September 1958: New Zealand J. Sci., v. 4(1), p. 162-188.

Perch-Nielsen, K. 1969. Die Coccolithen einiger Danischer Maastrichtien-und Danienlokalitaten: Medd. Dansk Geol. Forening, v. 19, p. 51-67.

Rasmussen, H. W., 1961. Echinoid and crustacean burrows and their diagenetic significance in the Maastrichtian-Danian of Stevns Klint, Denmark: Lethaia, v. 4, p. 191-216.

Roth, P. H., Baumann, P., and Bertolino, V., 1971. Late Eocene-Oligocene calcareous nannoplankton from Central and Northern Italy: Plank. Conf., 2nd, Roma 1970, Proc., p. 1069-1097.

Scott, G. H., 1972. *Globigerinoides* from Escornebeou (France) and the basal Miocene *Globigerinoides* Datum: New Zealand J. Geol. Geophys., v. 15(2), p. 287-295.

Stanton, B. R., 1969. Hydrological observations across the Tropical Convergence north of New Zealand: New Zealand J. Marine Freshwater Res., v. 3(1), p. 124-146.

Takayama, T., 1972. A note on the distribution of *Braarudosphaera bigelowi* (Gran & Braarud) Deflandre in the bottom sediments of Sendai Bay, Japan: Paleont. Soc. Japan Trans. Proc., n.s. 87, p. 429-435.

Vangerow, E. F. and Schloemer, W., 1967. Vergleich des "Vetschauer-kalkes" der Aachener Kreide mit dem Kreide-profil von Sud-Limburg anhand von coccolithen: Geol. Mijnbouw, v. 46, p. 453-458.

Wellman, P., McElhinny, M. W., and McDougall, I., 1969. On the polar-wander path for Australia during the Cenozoic: Roy. Astr. Soc. Geophys. J., v. 18 p. 371-395.

Wise, S. W., 1972. Calcite overgrowths on calcareous nannofossils: A taxonomic irritant and a key to the formation of chalk: Geol. Soc. Am. Abstr. Progr., 4(2), p. 115-116.

Worsley, T. and Martini, E., 1970. Late Maastrichtian nannoplankton provinces: Nature, v. 225(5239), p. 1242-1243.

## PLATE 1

Scanning electron micrographs of 210-5-CC (coarse fraction);
*Pseudoemiliania lacunosa* Zone, Pleistocene 1/3.

Figure 1        Assemblage; 1100X at 0°, PEL S847/24.

Figure 2        Assemblage; 1100X at 30°, PEL S846/13.

Figure 3        Assemblage (compare with Figure 1); 1700X at 0°, PEL S847/25. Note: C = Calcareous sponge spicule, M = *Micrascidites vulgaris* Deflandre & Deflandre-Rigaud, P = Planktonic microforaminifera, T = *Thoracosphaera heimii* (Lohmann) Kamptner.

Figure 4        Assemblage; 2700X at 0°, PEL S847/20.

Figure 5        Unknown prolate nannosphere, side view; 7000X at 30°, PEL S847/16.

Figure 6        Unknown prolate nannosphere, apertural view; 9500X at 74°, PEL S846/17.

PLATE 1
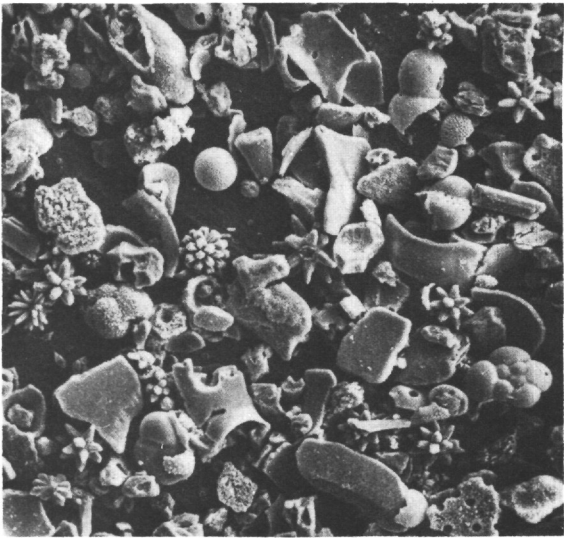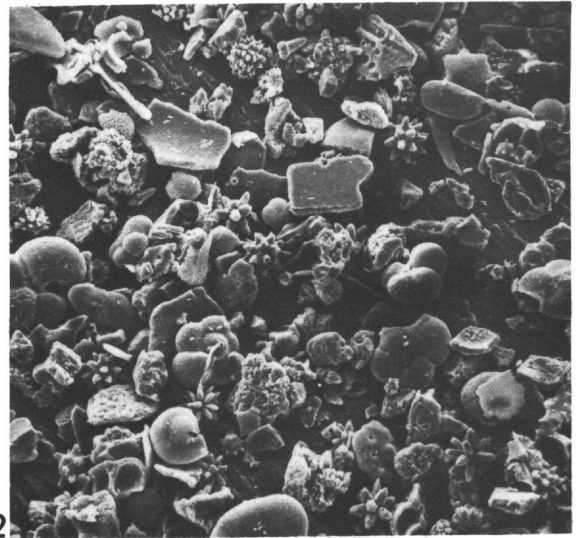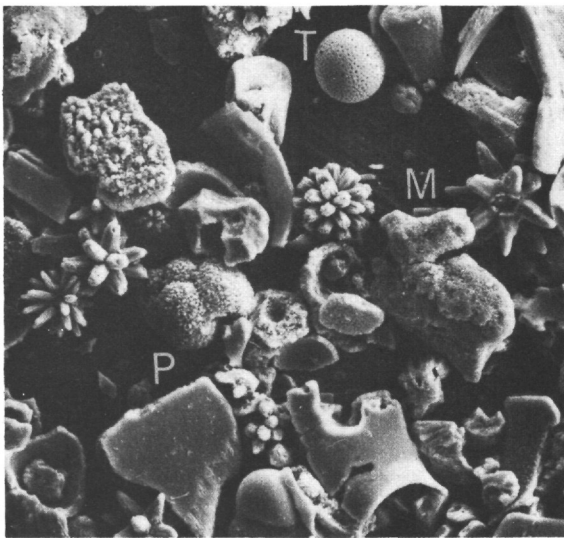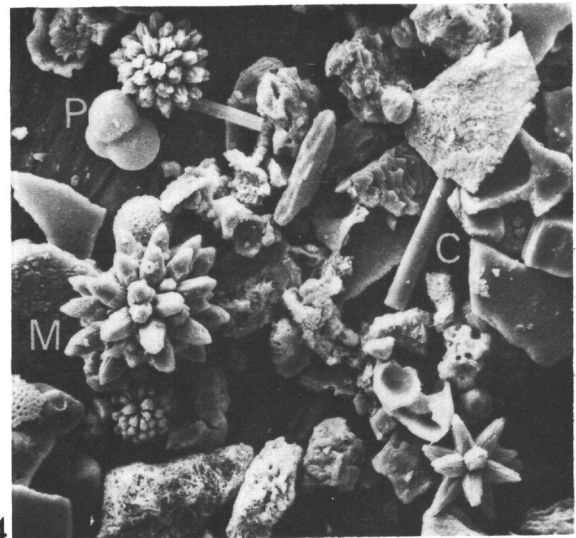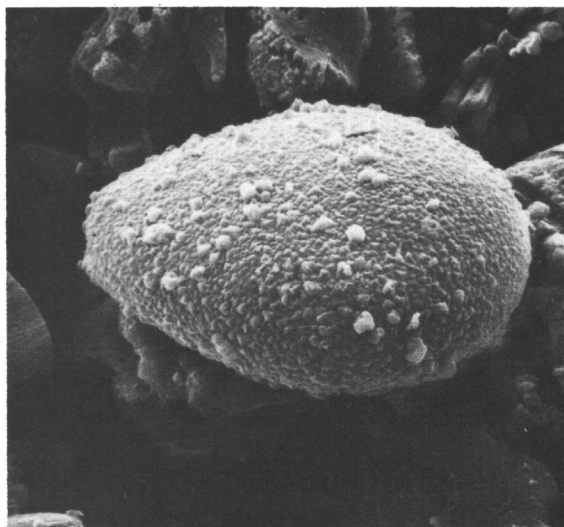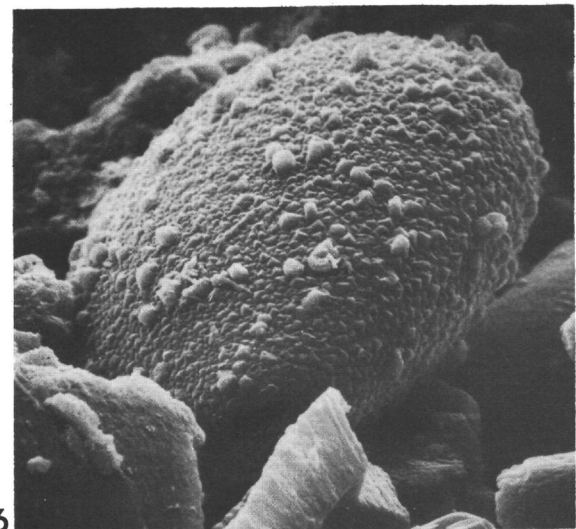
## PLATE 2

Scanning electron micrographs of 210-5-CC (coarse fraction);
*Pseudoemiliania lacunosa* Zone, Pleistocene 1/3.

Figure 1
*Micrascidites vulgaris* Deflandre and Deflandre-Rigaud (= M), *Thoracosphaera heimii* (Lohmann) Kamptner (= H) and *T. imperforata* Kamptner (= I) nanno-spheres; 6500X at 30°, PEL S904/3.

Figure 2
*Micrascidites vulgaris* Deflandre and Deflandre-Rigaud; 9000X at 0°; PEL S847/32.

Figure 3
*Micrascidites vulgaris* Deflandre and Deflandre-Rigaud; 12000X at 30°, PEL S904/1.

Figure 4
*Micrascidites vulgaris* Deflandre and Deflandre-Rigaud; 15000X at 30°, PEL S847/14.

Figure 5
*"Scyphosphaera"* cf. *apsteini* Lohmann (an alternative name is *Pontosphaera discopora* Schiller), oblique side view of lopodolith, and a partial, apertural, view of *Thoracosphaera heimii* (Lohmann) Kampter; 15000X at 0°, PEL S847/30.

Figure 6
*"Scyphosphaera"* cf. *apsteini* Lohmann, oblique close-up view of proximal end of lopodolith; 37000X at 0°, PEL S846/28.

**PLATE 2**
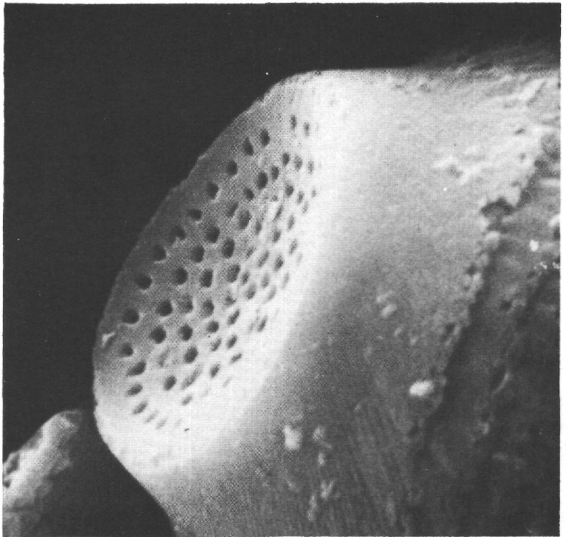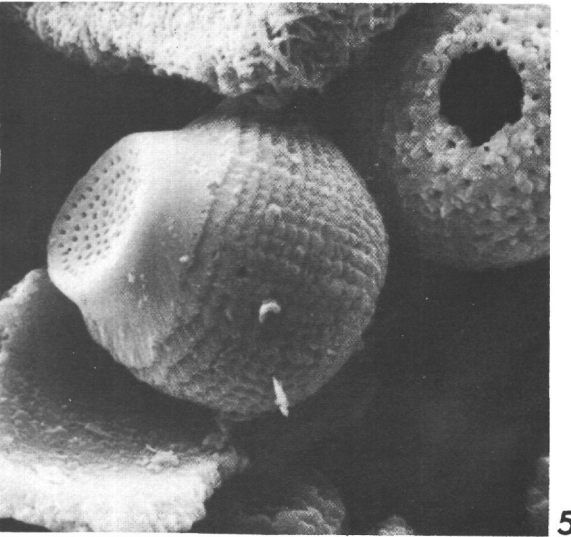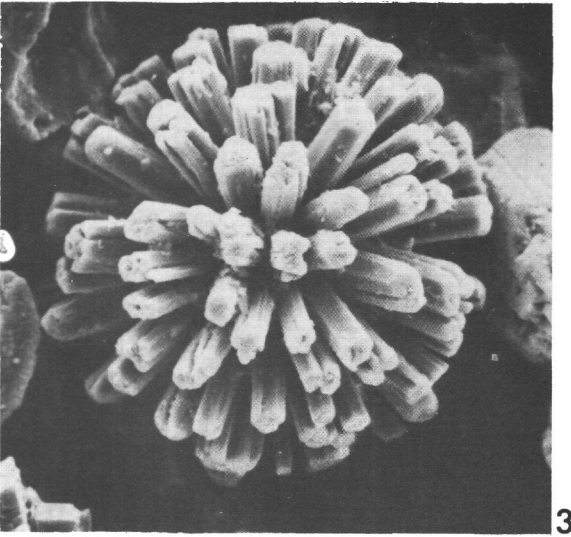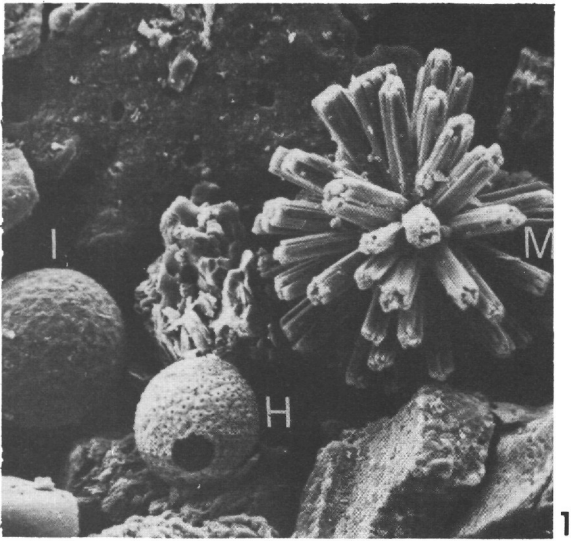
PLATE 3

Scanning electron micrographs of 210-5-CC (coarse fraction); *Pseudoemiliania lacunosa* Zone; Pleistocene 1/3.

Figure 1    *Thoracosphaera imperforata* Kamptner (cf Plate 2, Figure 1), side view; 23000X at 30°; PEL S904/2.

Figure 2    *Thoracosphaera* n. sp. (only specimen observed), side view; 10000X at 0°, PEL S847/33.

Figure 3    *Thoracosphaera* n. sp., close-up side view showing nannosphere ultrastructure; 23000X at 0°, PEL S847/34.

Figure 4    *Thoracosphaera heimii* (Lohmann) Kamptner; close-up side view showing nannosphere ultrastructure; 34000X at 0°, PEL S847/23.

Figure 5    *Thoracosphaera heimii* (Lohmann) Kamptner, side view; 18000X at 0°, PEL S847/22.

Figure 6    *Thoracosphaera heimii* (Lohmann) Kamptner, oblique apertural view; 18000X at 0°, PEL S847/26.

PLATE 3
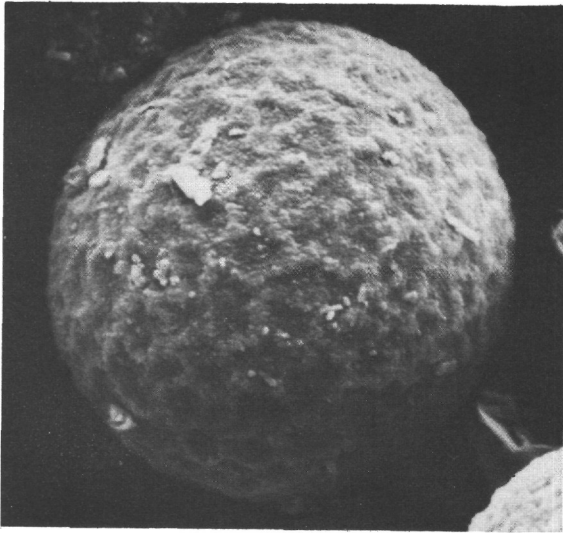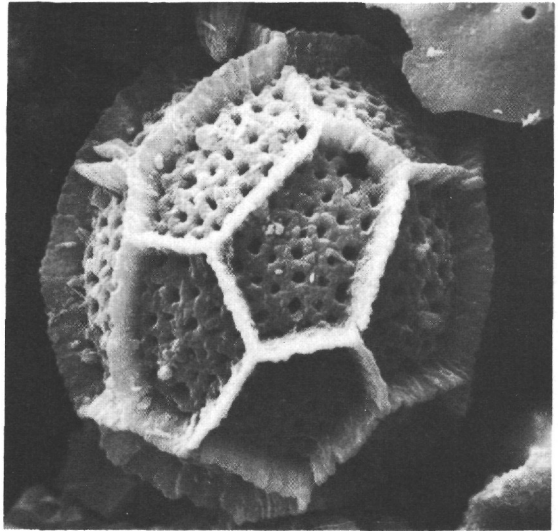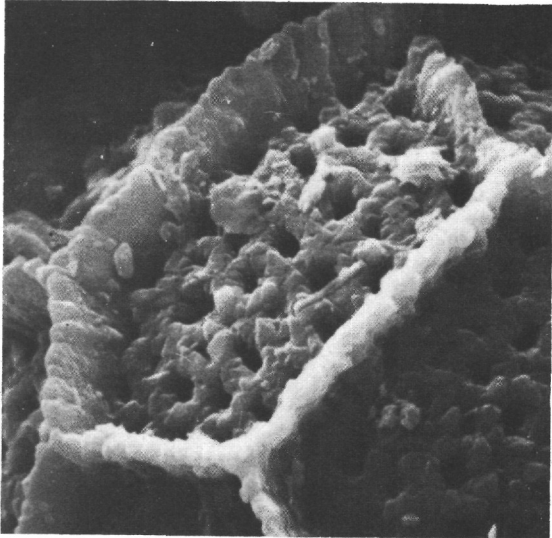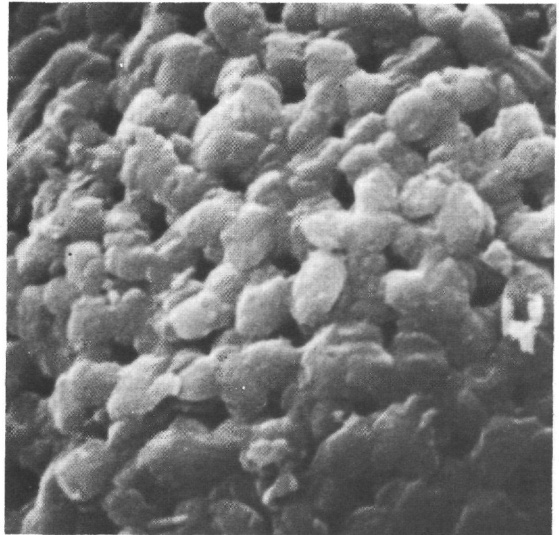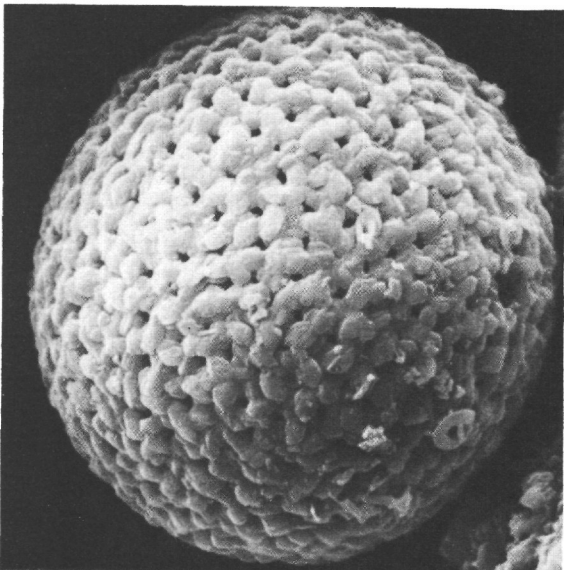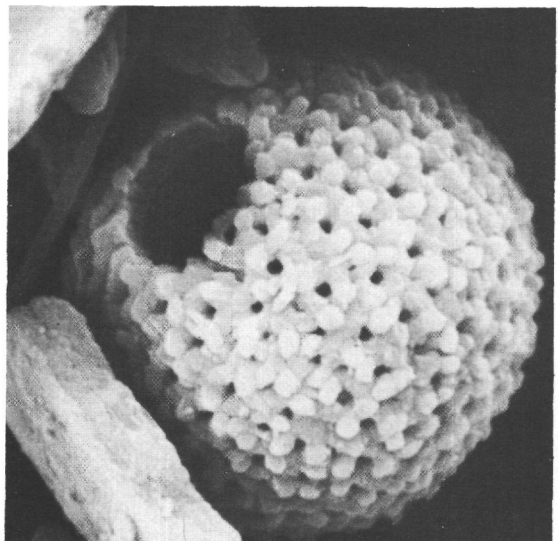
## PLATE 4

Scanning (S) and transmission electron micrographs of
important Mesozoic-Cenozoic boundary species.

Figure 1        *Cruciplacolithus tenuis* (Stradner) Hay and Mohler,
                proximal view; 6000X, PEL 2542/2; 208-30-4, 29
                cm, *Prinsius martinii* Zone, Early Paleocene 4/5.

Figure 2        *Hornibrookina teuriensis* Edwards, proximal view;
                8000X, PEL 2537/5; 208-30-4, 29 cm, *Prinsius
                martinii* Zone, Early Paleocene 4/5.

Figure 3        *Chiasmolithus danicus* (Brotzen) Hay and Mohler,
                distal view; 37000X at 30°, PEL S729/32; 208-31-2,
                27 cm, *Prinsius martinii* Zone, Early Paleocene 4/5.

Figure 4        *Markalius astroporus* (Stradner) Hay and Mohler,
                oblique proximal view; 39000X at 30°, PEL S729/30;
                208-31-2, 27 cm, *Prinsius martinii* Zone, Early
                Paleocene 4/5.

Figure 5        Assemblage; 9500X at 45°, PEL S730/4; 208-34-1,
                127 cm, *Nephrolithus frequens* Zone (lower),
                Maastrichtian 2/3.

Figure 6        *Nephrolithus frequens* Gorka, distal view; 50000X at
                45°, PEL S730/5; 208-34-1, 127 cm, *Nephrolithus
                frequens* Zone (lower), Maastrichtian 2/3.

PLATE 4
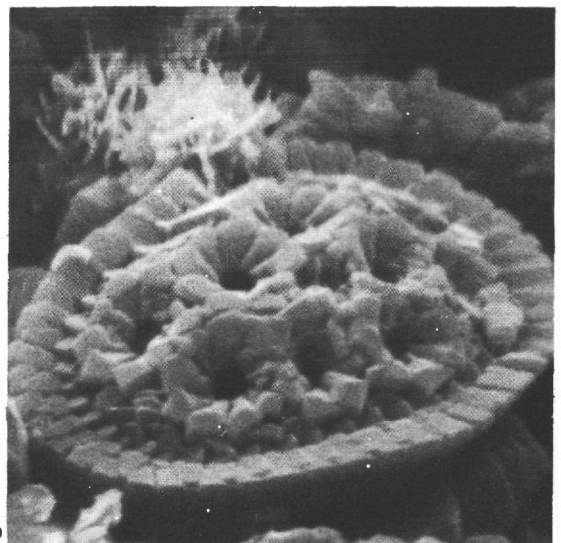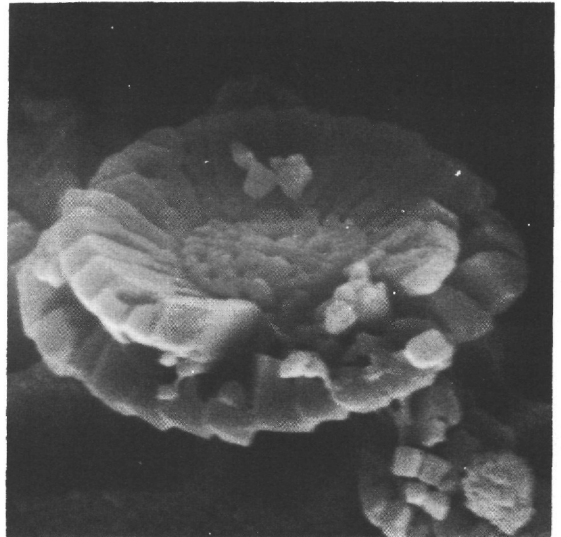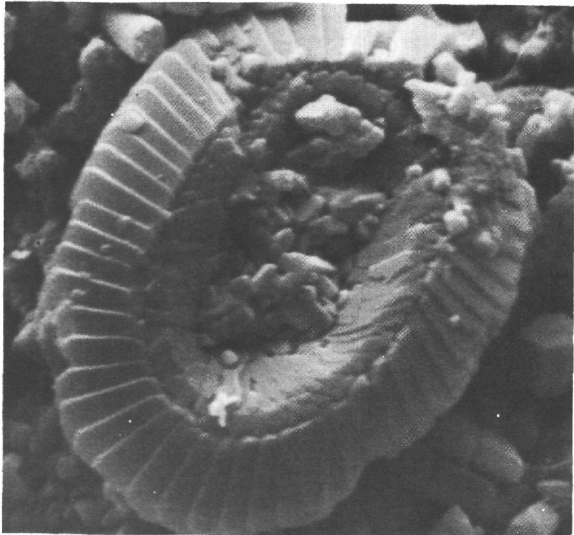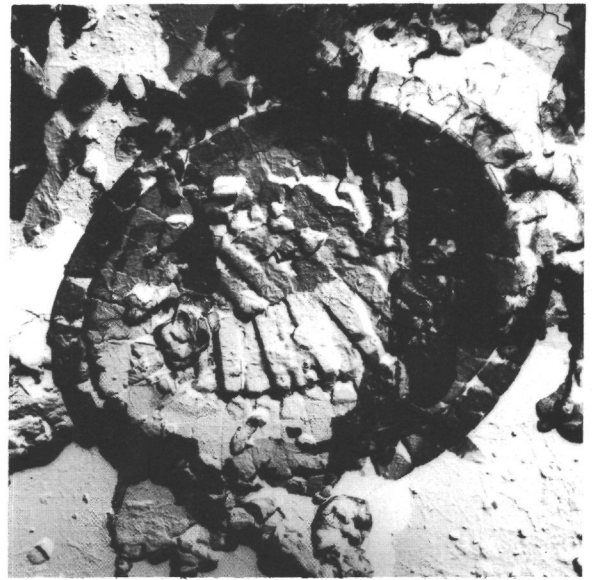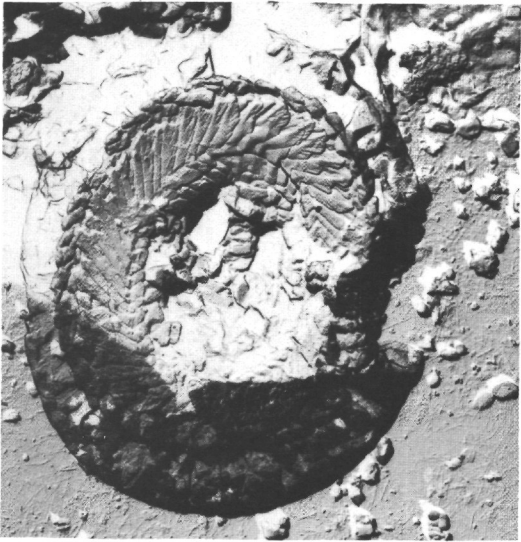
## PLATE 5

Transmission electron micrographs of Paleogene Coccolithaceae

Figure 1      *Chiasmolithus expansus* (Bramlette and Sullivan) Gartner, distal view; 4800X, PEL 2540/28; 207A-20-1, 25 cm, *Chiphragmalithus cristatus* Zone (lower, mid Eocene 3/7.

Figure 2      *Chiasmolithus expansus* (Bramlette and Sullivan) Gartner, proximal view; 6000X, PEL 2540/25; 207A-20-1, 25 cm, *Chiphragmalithus cristatus* Zone (lower), mid Eocene 3/7.

Figure 3      *Chiasmolithus grandis* (Bramlette and Riedel) Radomski, distal view; 3700X, PEL 2539/16; 207A-25-2, 25 cm, *Discoaster lodoensis* Zone, Early Eocene 4/5.

Figure 4      *Chiasmolithus grandis* (Bramlette and Riedel) Radomski, distal view; 3700X, PEL 2539/6; 207A-25-2, 25 cm, *Discoaster lodoensis* Zone, Early Eocene 4/5.

Figure 5      *Chiasmolithus bidens* (Bramlette and Sullivan) Hay and Mohler, distal view: 6000X, PEL 2541/19; 207A-26-4, 100 cm, *Discoaster multiradiatus* Zone, Late Paleocene 1/3.

Figure 6      *Chiasmolithus bidens* (Bramlette and Sullivan) Hay and Mohler, proximal view; 7500X, PEL 2537/7; 208-30-4, 29 cm, *Prinsius martinii* Zone, Early Paleocene 4/5.

PLATE 5
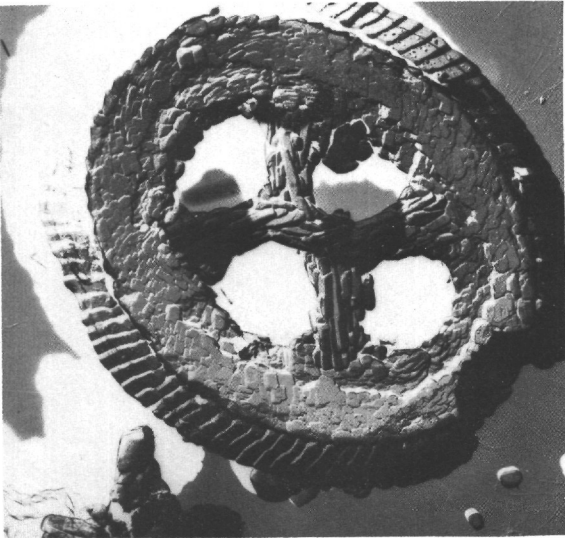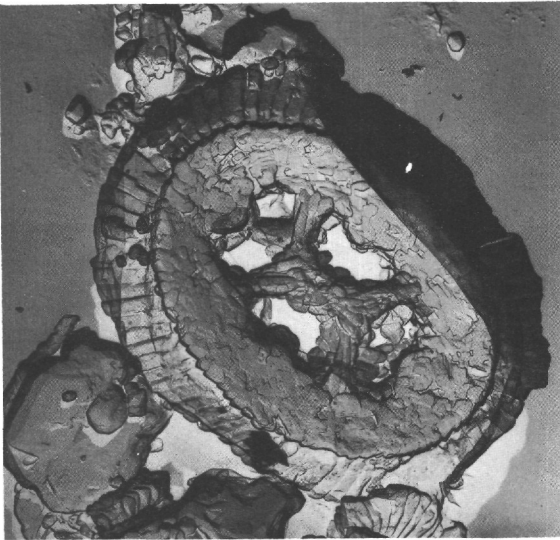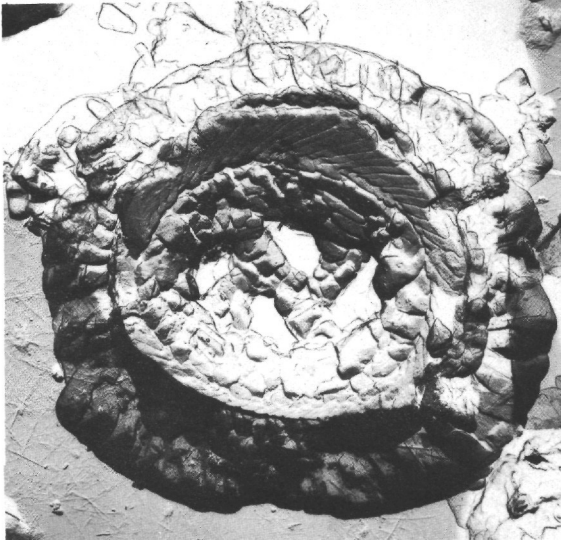
PLATE 6

Transmission electron micrographs of Paleogene Coccolithaceae

Figure 1      *Chiasmolithus solitus* (Bramlette and Sullivan) Locker, distal view; 4800X, PEL 2540/27; 207A-20-1, 25 cm, *Chiphragmalithus cristatus* Zone (lower), mid Eocene 3/7.

Figure 2      *Chiasmolithus solitus* (Bramlette and Sullivan) Locker, proximal view; 6000X, PEL 2541/7; 207A-20-1, 25 cm, *Chiphragmalithus cristatus* Zone (lower), mid Eocene 3/7.

Figure 3      *Coccolithus eopelagicus* (Bramlette and Riedel) Bramlette and Sullivan, distal view; 4800X, PEL 2544/27; 207A-9-6, 25 cm, *Chiasmolithus oamaruensis* Zone, Late Eocene 2/5.

Figure 4      *"Ericsonia" ovalis* Black (= *Coccolithus muiri* Black), coccosphere; 6000X, PEL 2539/17; 207A-25-2, 25 cm, *Discoaster lodoensis* Zone, Early Eocene 4/5.

Figure 5      *"Ericsonia" ovalis* Black, distal view; 10000X, PEL 2539/1; 207A-25-2, 25 cm, *Discoaster lodoensis* Zone, Early Eocene 4/5.

Figure 6      *"Ericsonia" ovalis* Black, distal view; 10000X, PEL 2541/17; 207A-26-4, 100 cm, *Discoaster multiradiatus* Zone, Late Paleocene 1/3.

PLATE 6
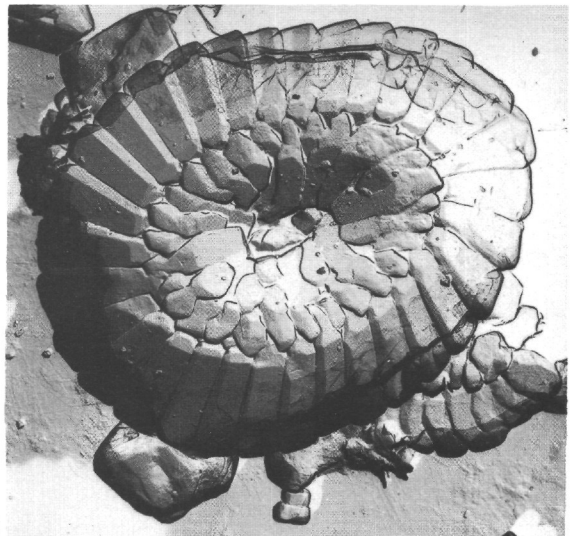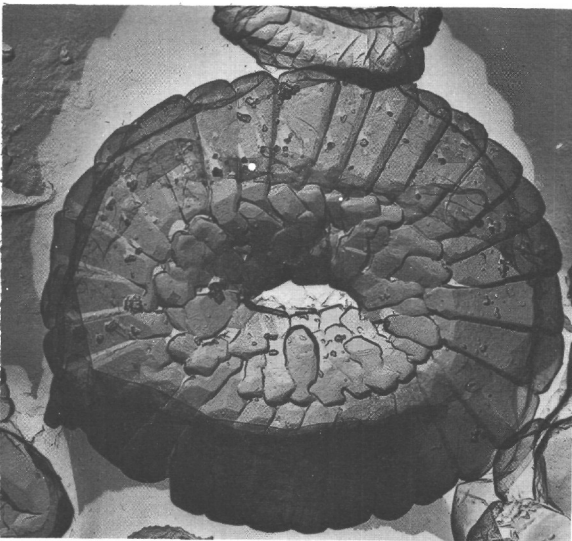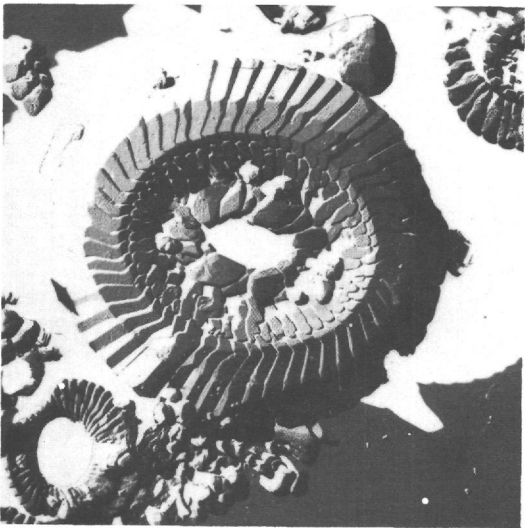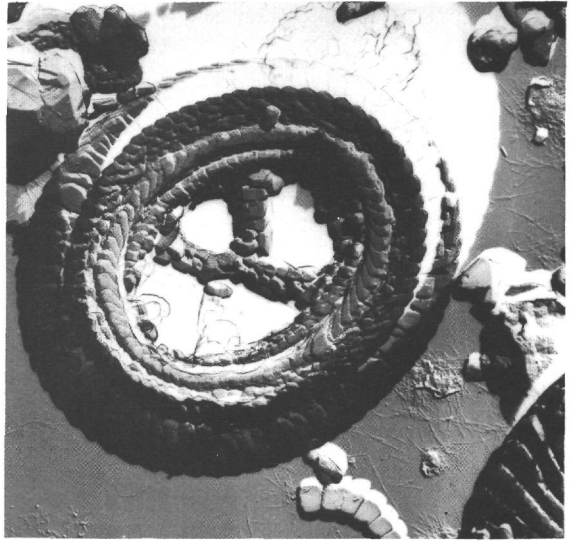
## PLATE 7

Transmission electron micrographs of Paleogene Coccolithaceae.

Figure 1    *"Cyclococcolithina" formosa* (Kamptner) Wilcoxon, distal view; 6000X, PEL 2540/20; 207A-20-1, 25 cm, *Chiphragmalithus cristatus* Zone (lower), mid Eocene 3/7.

Figure 2    *"Cyclococcolithina" formosa* (Kamptner) Wilcoxon, distal view; 6000X, PEL 2540/21; 207A-20-1, 25 cm, *Chiphragmalithus cristatus* Zone (lower), mid Eocene 3/7.

Figure 3    *"Cyclococcolithina" formosa* (Kamptner) Wilcoxon, distal view; 4800X, PEL 2540/1; 207A-24-1, 25 cm, *Reticulofenestra dictyoda* Zone (upper), mid Eocene 1/7.

Figure 4    *"Cyclococcolithina" formosa* (Kamptner) Wilcoxon, distal view; 6000X, PEL 2539/28; 207A-24-1, 25 cm, *Reticulofenestra dictyoda* Zone (upper), mid Eocene 1/7.

Figure 5    *"Cyclococcolithina" formosa* (Kamptner) Wilcoxon, proximal view; 7500X, PEL 2539/22; 207A-24-1, 25 cm, *Reticulofenestra dictyoda* Zone (upper), mid Eocene 1/7.

Figure 6    *Coccolithus* sp., distal view; 15000X, PEL 2542/25; 209-30-CC, combined *Reticulofenestra hampdenensis* and *Discoaster distinctus* zones, mid Eocene 6/7.

PLATE 7
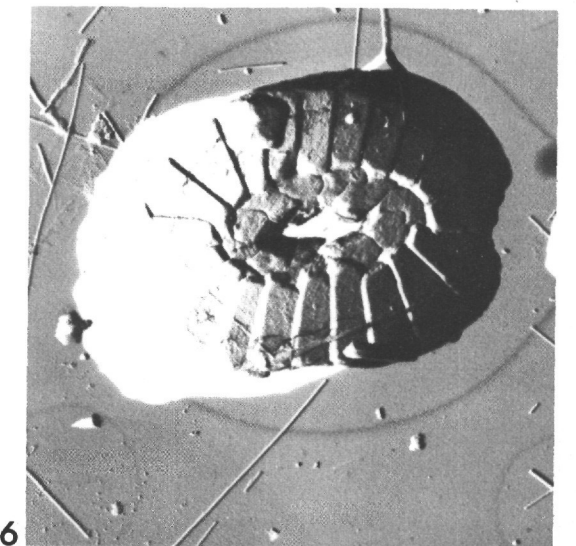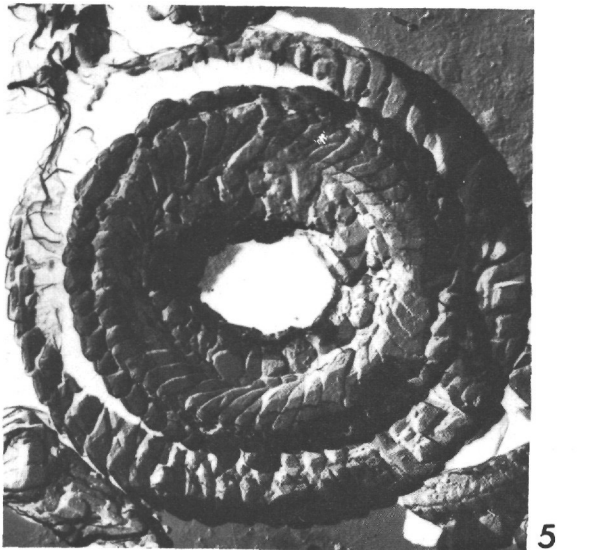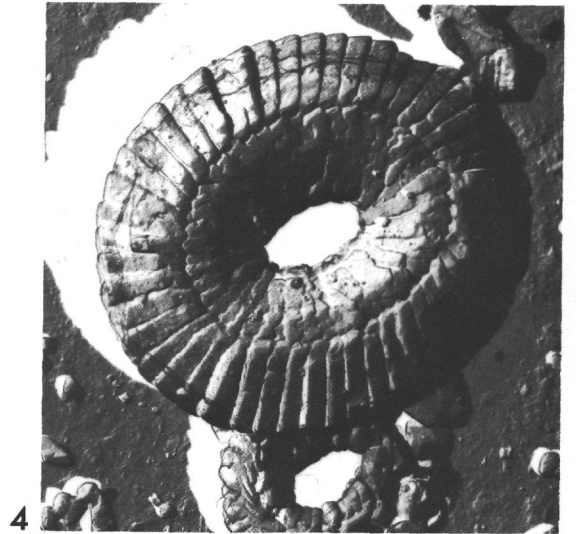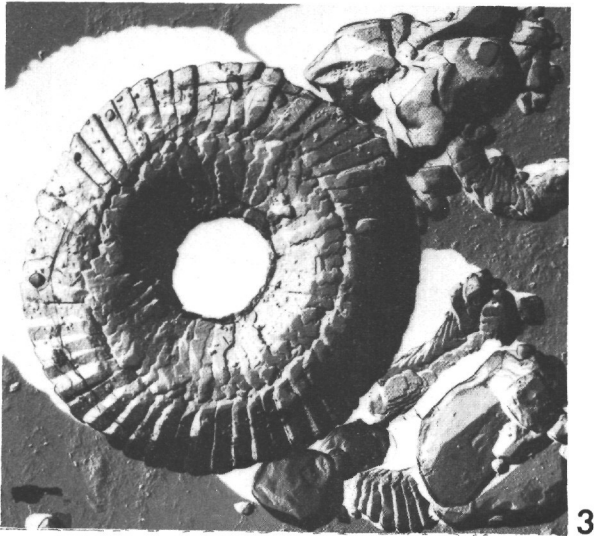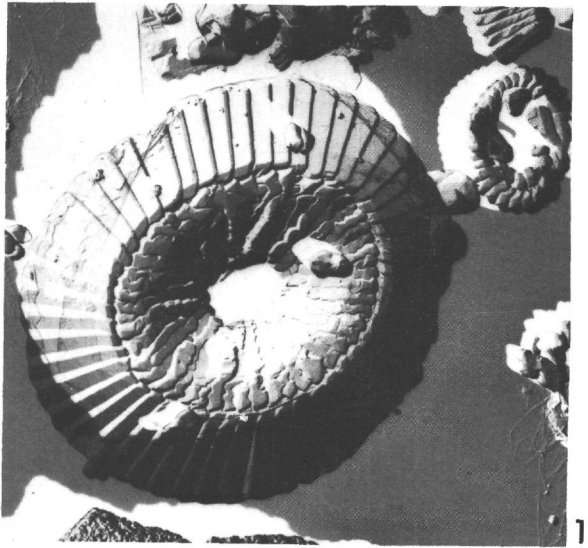
PLATE 8

Transmission electron micrographs of Paleogene
Coccolithaceae and Pontosphaeraceae.

Figure 1      *Coccolithus* sp., distal view; 10000X, PEL 2543/3; 209-30-CC, combined *Reticulofenestra hampdenensis* and *Discoaster distinctus* zones, mid Eocene 6/7.

Figure 2      *Helicopontosphaera lophota* (Bramlette and Sullivan) Bukry, proximal view; 10000X, PEL 2540/32; 207A-20-1, 25 cm, *Chiphragmalithus cristatus* Zone (lower), mid Eocene 3/7.

Figure 3      *Helicopontosphaera seminulum* (Bramlette and Sullivan) Stradner, proximal view; 4800X, PEL 2539/9; 207A-25-2, 25 cm, *Discoaster lodoensis* Zone, Early Eocene 4/5.

Figure 4      *Discolithina multipora* (Kamptner ex Deflandre) Martini, distal view of a shallow lopodolith (*"Crassapontosphaera"*); 10000X, PEL 2542/27; 209-30-CC, combined *Reticulofenestra hampdenensis* and *Discoaster distinctus* zones, mid Eocene 6/7.

Figure 5      *Discolithina pulchra* (Deflandre) Levin, distal view of a discolith; 13000X, PEL 2542/29; 209-30-CC, combined *Reticulofenestra hampdenensis* and *Discoaster distinctus* zones, mid Eocene 6/7.

Figure 6      *Discolithina pulcheroides* (Sullivan) Levin and Joerger ?, proximal view, 13000X, PEL 2543/1; 209-30-CC, combined *Reticulofenestra hampdenensis* and *Discoaster distinctus* zones, mid Eocene 6/7.

PLATE 8
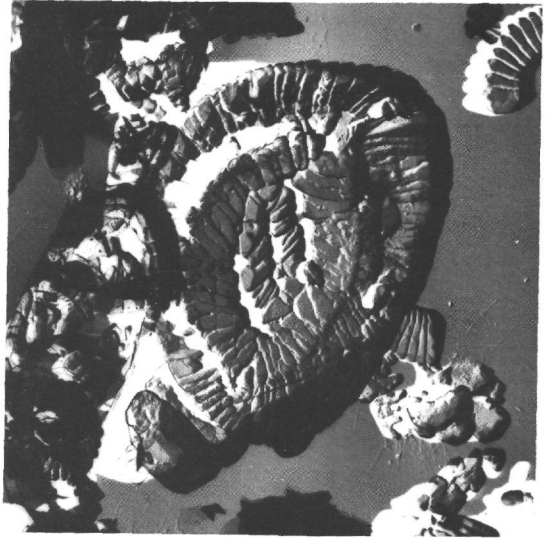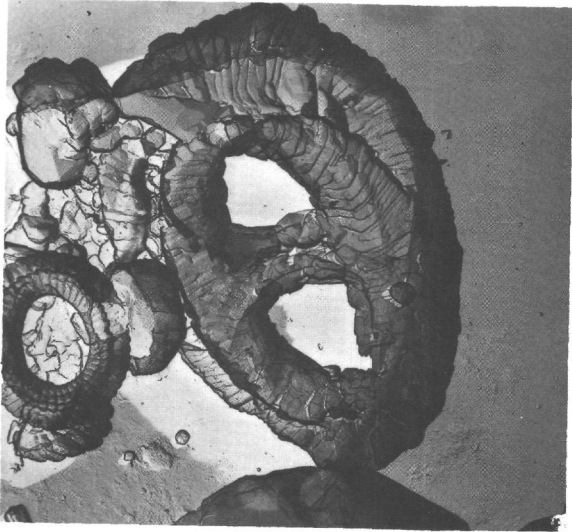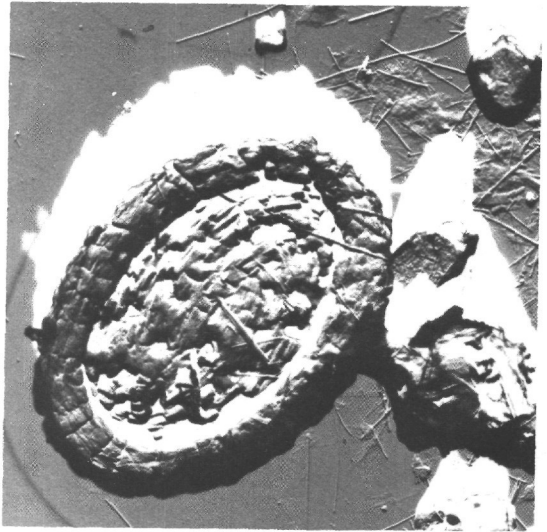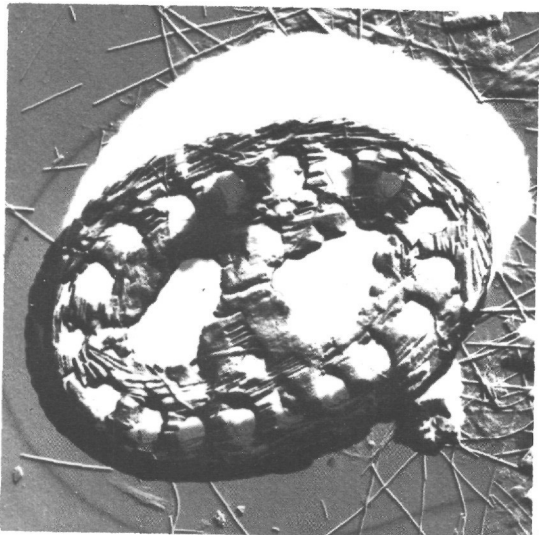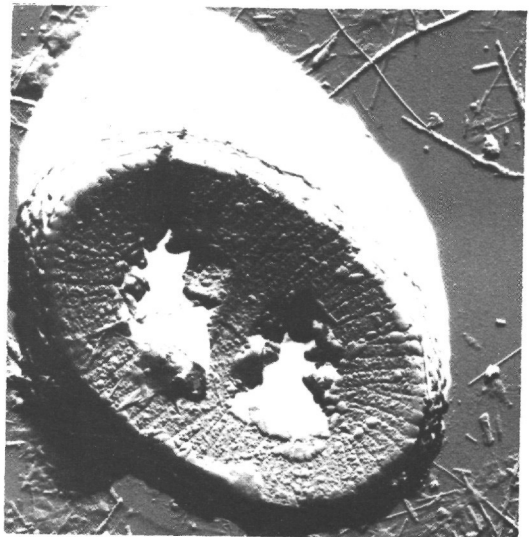
PLATE 9

Transmission electron micrographs of Paleogene Coccolithaceae?
and Prinsiaceae.

Figure 1    *Hornibrookina* n. sp., distal view; 10000X, PEL
            2536/21; 207A-26-4, 100 cm, *Discoaster multi-
            radiatus* Zone, Late Paleocene 1/3.

Figure 2    *Hornibrookina* n. sp., proximal view; 13000X, PEL
            2541/22; 207A-26-4, 100 cm, *Discoaster multi-
            radiatus* Zone, Late Paleocene 1/3.

Figure 3    *Hornibrookina* n. sp., distal view showing the
            convexity characteristic of this species; 13000X, PEL
            2541/28; 207A-26-4, 100 cm, *Discoaster multi-
            radiatus* Zone, Late Paleocene 1/3.

Figure 4    *Ellipsolithus distichus* (Bramlette and Sullivan)
            Sullivan, proximal view; 6000X, PEL 2540/26;
            207A-20-1, 25 cm, *Chiphragmalithus cristatus* Zone
            (lower), mid Eocene 3/7.

Figure 5    *Cyclicargolithus* cf *floridanus* (Roth and Hay) Bukry,
            distal view; 10000X, PEL 2544/28; 207A-9-6, 25 cm,
            *Chiasmolithus oamaruensis* Zone, Late Eocene 2/5.

Figure 6    *Reticulofenestra hampdenensis* Edwards, distal view;
            10000X, PEL 2544/19; 209-30-CC, combined *Reticu-
            lofenestra hampdenensis* and *Discoaster distinctus*
            zones, mid Eocene 6/7.

PLATE 9
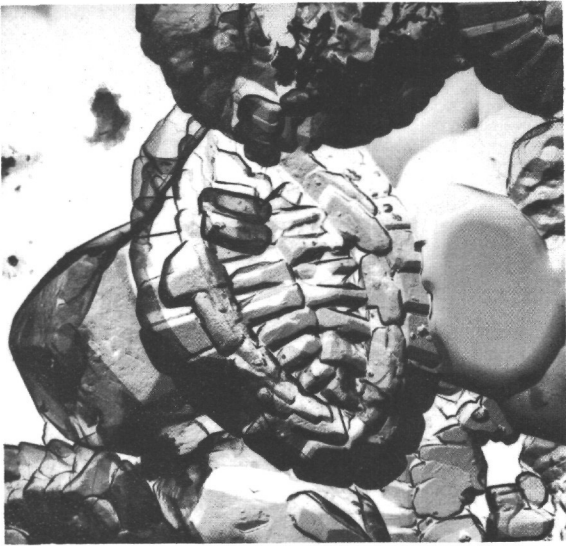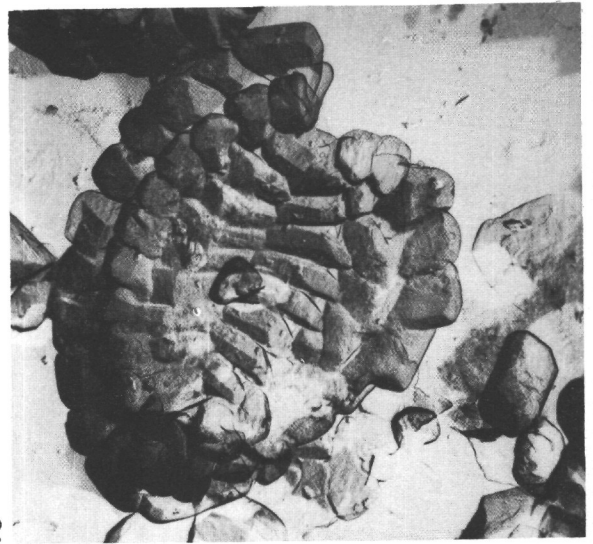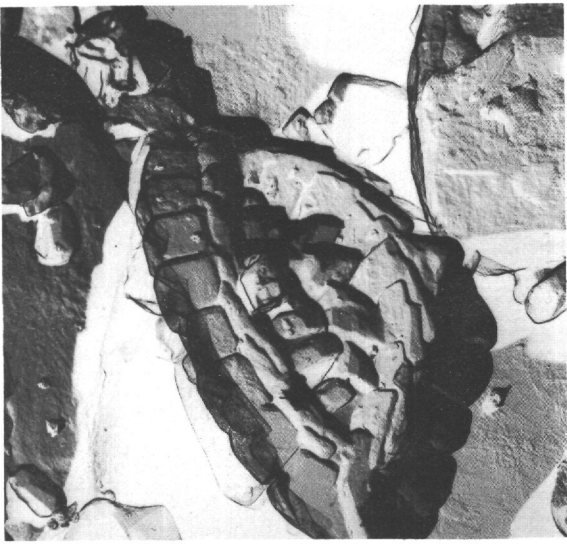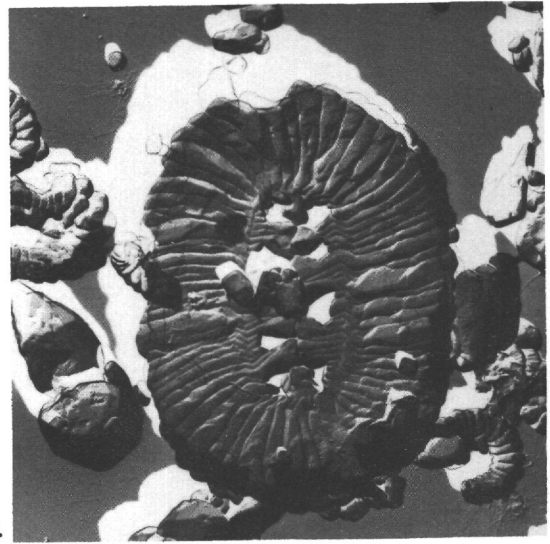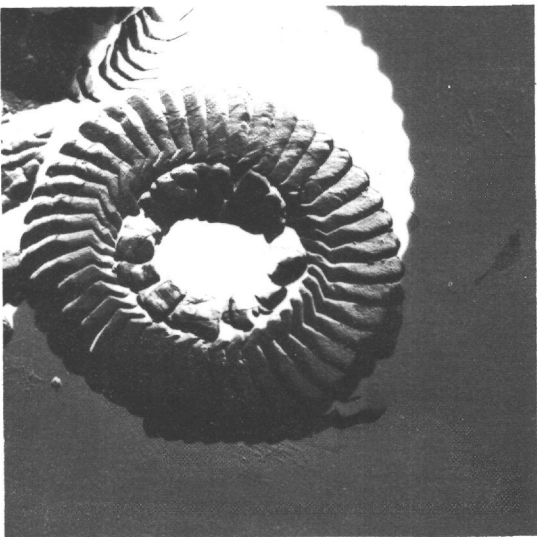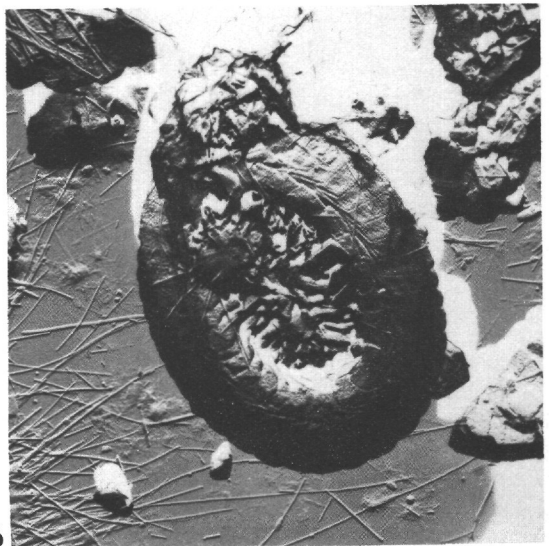
## PLATE 10

Transmission electron micrographs of Eocene Prinsiaceae.

Figure 1      *Reticulofenestra bisecta* (Hay, Mohler and Wade) Roth (= *R. scissura* Hay, Mohler and Wade), distal view; 4800X, PEL 2542/16; 207A-9-6, 25 cm, *Chiasmolithus oamaruensis* Zone, Late Eocene 2/5.

Figure 2      *Reticulofenestra placomorpha* (Kamptner) Stradner (alternative name: *R. umbilica* (Levin) Martini and Ritzkowski), proximal view of "late" form; 4800X, PEL 2542/15; 207A-9-6, 25 cm, *Chiasmolithus oamaruensis* Zone, Late Eocene 2/5.

Figure 3      *Reticulofenestra placomorpha* (Kamptner) Stradner, distal view of "early" form; 4800X, PEL 2543/8; 207A-11-2, 30 cm, combined *Reticulofenestra hampdenensis* and *Discoaster distinctus* Zones, mid Eocene 6/7.

Figure 4      *Reticulofenestra placomorpha* (Kamptner) Stradner, proximal view of "early" form; 4800X, PEL 2542/13; 207A-11-2, 30 cm, combined *Reticulofenestra hampdenensis* and *Discoaster distinctus* Zones, mid Eocene 6/7.

Figure 5      *Reticulofenestra dictyoda* (Deflandre and Fert) Stradner, distal view; 7500X, PEL 2540/16; 207A-20-1, 25 cm, *Chiphragmalithus cristatus* Zone (lower), mid Eocene 3/7.

Figure 6      *Reticulofenestra dictyoda* (Deflandre and Fert) Stradner, proximal view; 7500X, PEL 2540/19; 207A-20-1, 25 cm, *Chiphragmalithus cristatus* Zone (lower), mid Eocene 3/7.

PLATE 10
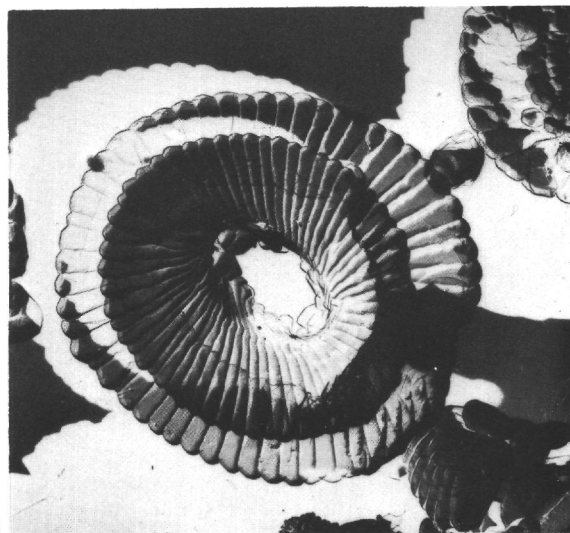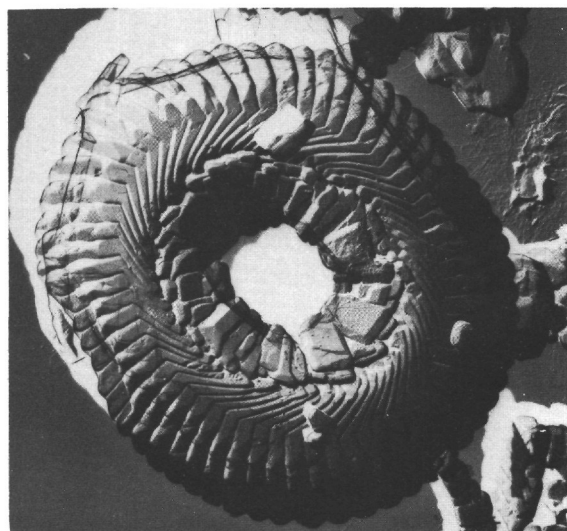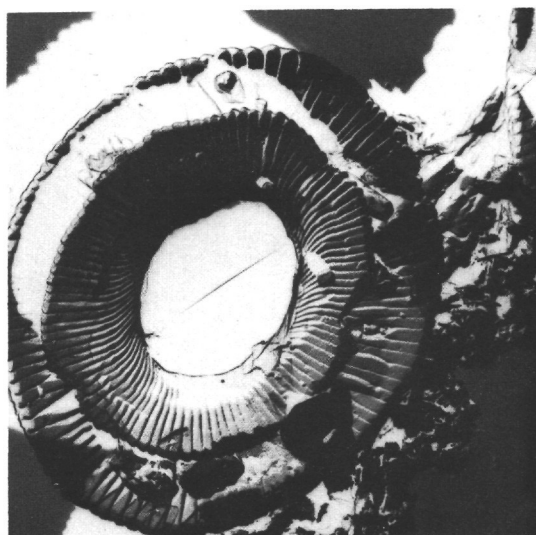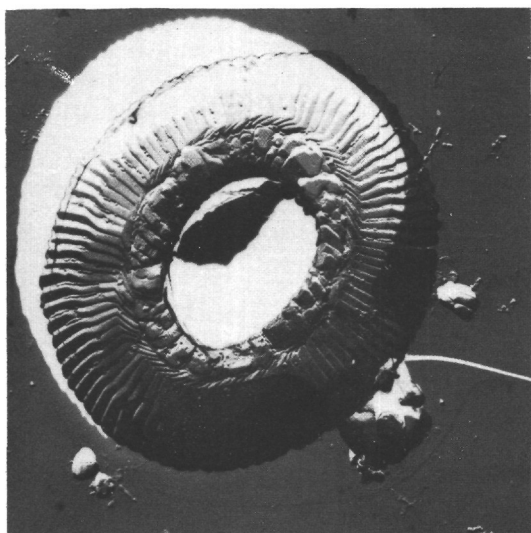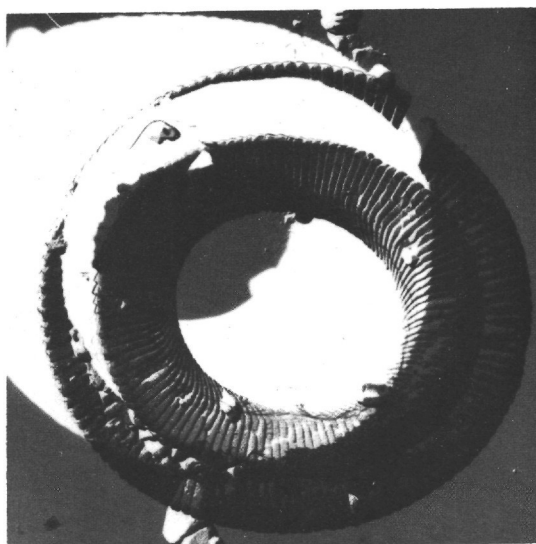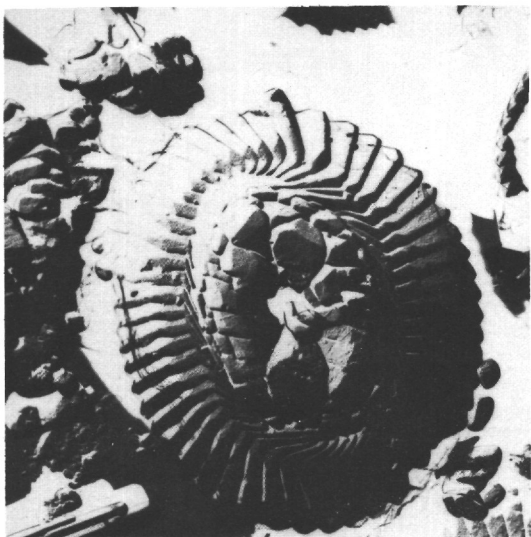
## PLATE 11

Transmission electron micrographs of Paleocene Prinsiaceae
and Calciosoleniaceae.

Figure 1    *Prinsius martinii* (Perch-Nielsen) Haq, distal view; 15000X, PEL 2542/10; 207A-27-2, 100 cm, *Heliolithus kleinpelli* Zone, mid Paleocene 2/3.

Figure 2    *Toweius eminens* (Bramlette and Sullivan) Perch-Nielsen, distal view; 10000X, PEL 2545/9; 207A-26-4, 100 cm, *Discoaster multiradiatus* Zone, Late Paleocene 1/3.

Figure 3    *Toweius craticulus* Hay and Mohler, distal view; 10000X, PEL 2541/16; 207A-26-4, 100 cm, *Discoaster multiradiatus* Zone, Late Paleocene 1/3.

Figure 4    *Toweius craticulus* Hay and Mohler, distal view; 10000X, PEL 2545/4; 207A-26-4, 100 cm, *Discoaster multiradiatus* Zone, Late Paleocene 1/3.

Figure 5    *Toweius tovae* Perch-Nielsen, distal view; 6000X, PEL 2545/12; 207A-26-4, 100 cm, *Discoaster multiradiatus* Zone, Late Paleocene 1/3.

Figure 6    *"Scapholithus" apertus* Hay and Mohler, plain view; 13000X, PEL 2545/7; 207A-26-4, 100 cm, *Discoaster multiradiatus* Zone, Late Paleocene 1/3.

PLATE 11
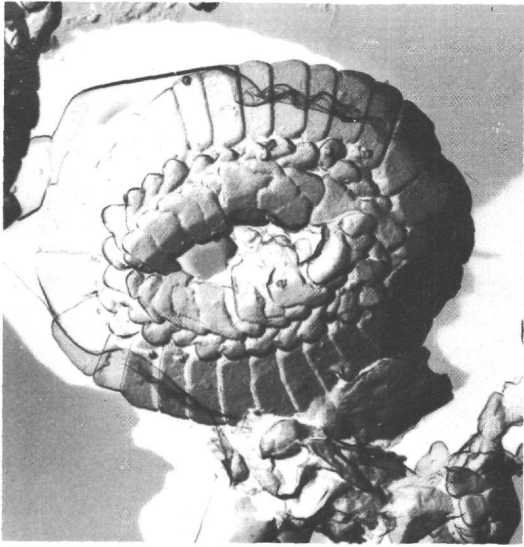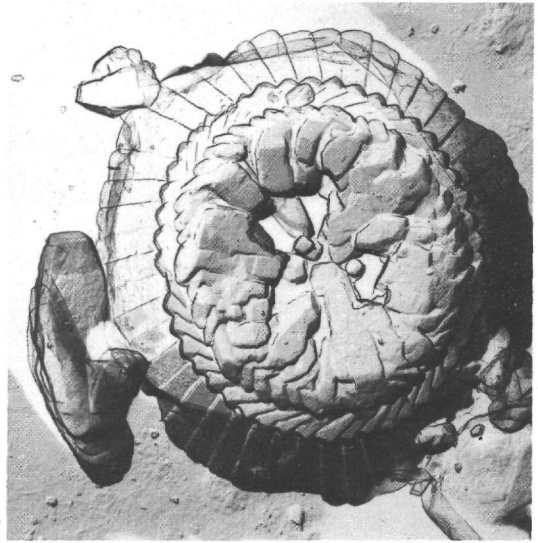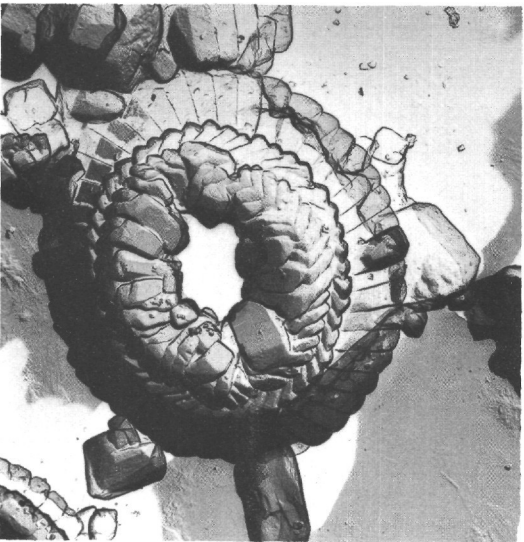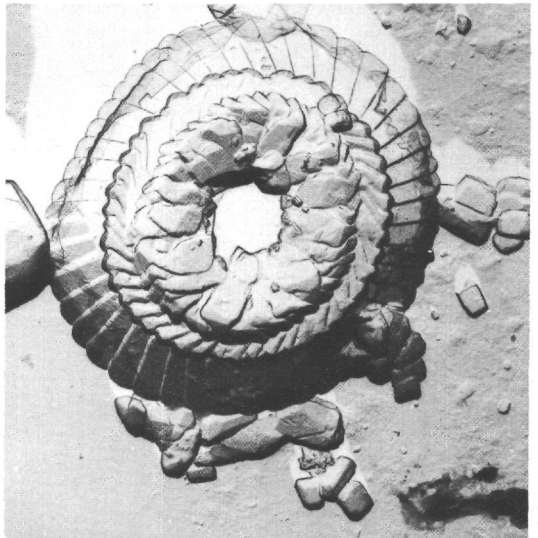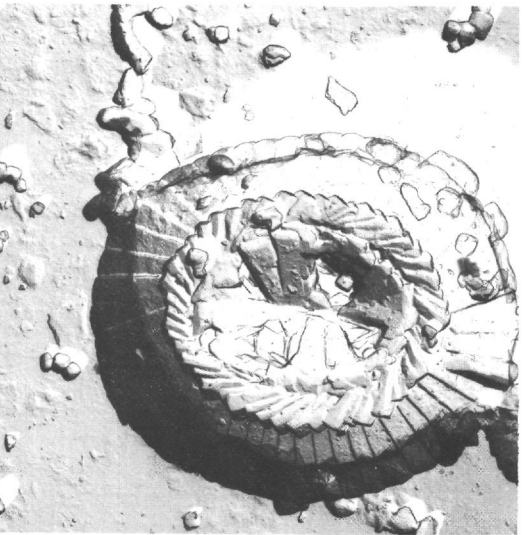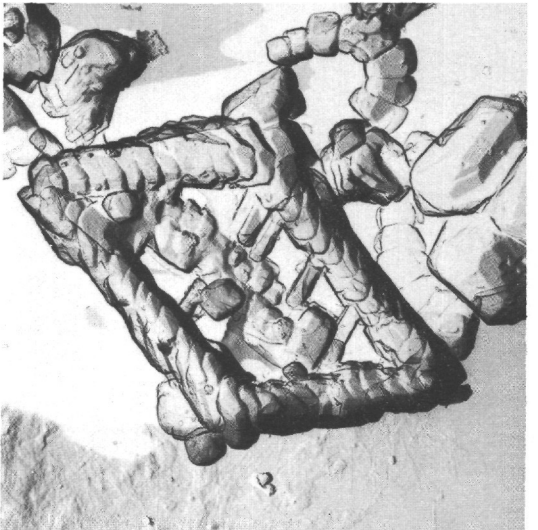
PLATE 12

Transmission electron micrographs of Paleogene Zygodiscaceae.

Figure 1    *Zygodiscus sigmoides* Bramlette and Sullivan, distal view; 7500X, PEL 2545/2; 207A-26-4, 100 cm, *Discoaster multiradiatus* Zone, Late Paleocene 1/3.

Figure 2    *Zygodiscus sigmoides* Bramlette and Sullivan, proximal view; 7500X, PEL 2541/13; 207A-26-4, 100 cm, *Discoaster multiradiatus* Zone, Late Paleocene 1/3.

Figure 3    *Zygodiscus sigmoides* Bramlette and Sullivan, oblique side view; 6000X, PEL 2541/11; 207A-26-4, 100 cm, *Discoaster multiradiatus* Zone, Late Paleocene 1/3.

Figure 4    *Neochiastozygus junctus* (Bramlette and Sullivan) Perch-Nielsen, proximal view?; 6000X, PEL 2542/8; 207A-27-2, 100 cm, *Heliolithus kleinpelli* Zone, mid Paleocene 2/3.

Figure 5    *Zygolithus dubius* Deflandre, plan view; 7500X, PEL 2540/31; 207A-20-1, 25 cm, *Chiphragmalithus cristatus* Zone (lower), mid Eocene 3/7.

Figure 6    *Zygolithus dubius* Deflandre, oblique plan view showing central "overgrowth," 10000X, PEL 2539/8; 207A-25-2, 25 cm, *Discoaster lodoensis* Zone, Early Eocene 4/5.

PLATE 12
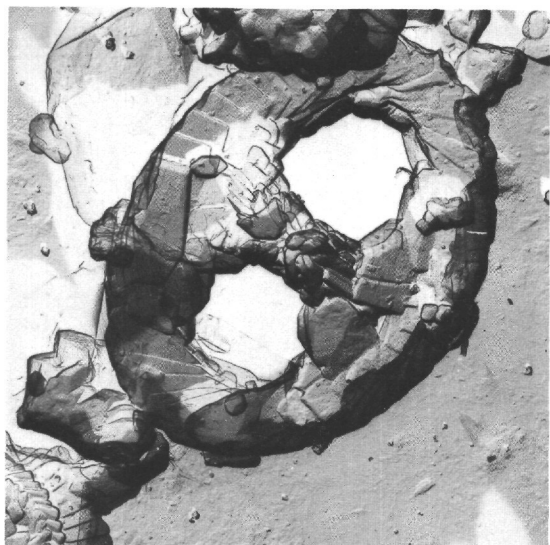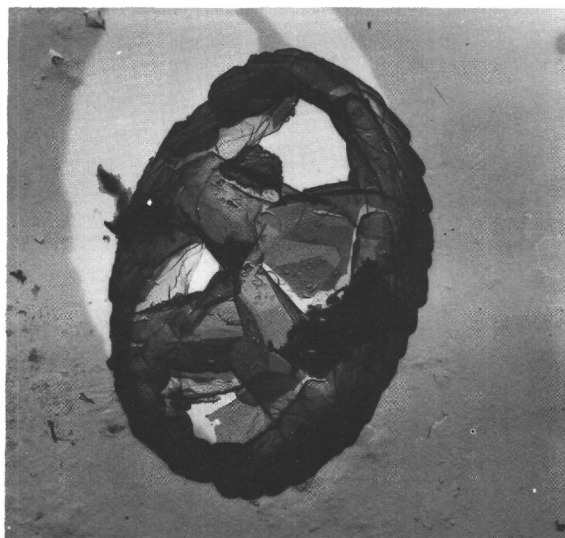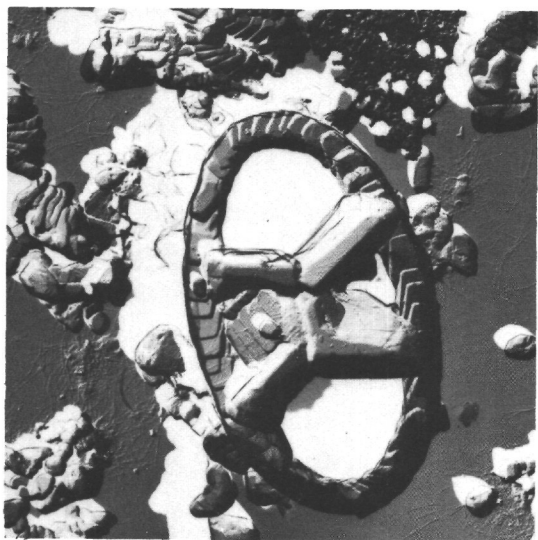
## PLATE 13

Transmission electron micrographs of Paleogene Calytrosphaeraceae
and Braarudosphaeraceae.

Figure 1    *Zygrhablithus bijugatus* Deflandre, side view of recrystallized specimen; 10000X, PEL 2540/22; 207A-20-1, 25 cm, *Chiphragmalithus cristatus* Zone (lower), mid Eocene 3/7.

Figure 2    *Zygrhablithus bijugatus* Deflandre, side view of disintegrating recrystallized specimen; 7500X, PEL 2539/12; 207A-25-2, 25 cm, *Discoaster lodoensis* Zone, Early Eocene 4/5.

Figure 3    *"Semihololithus" kerabyi* Perch-Nielsen, side view of a recrystallized specimen; 6000X, PEL 2541/18; 207A-26-4, 100 cm, *Discoaster multiradiatus* Zone, Late Paleocene 1/3.

Figure 4    *Braarudosphaera bigelowi* (Gran and Braarud) Deflandre, plan view; 4800X, PEL 2539/11; 207A-25-2, 25 cm, *Discoaster lodoensis* Zone, Early Eocene 4/5.

Figure 5    *Micrantholithus* sp.?, plan view (note imbricate arrangement of the segments); 7500X, PEL 2539/18; 207A-25-2, 25 cm, *Discoaster lodoensis* Zone, Early Eocene 4/5.

Figure 6    *Braarudosphaera discula* Bramlette and Sullivan, plan view of segment; 10000X, PEL 2543/6; 207A-11-2, 30 cm, combined *Reticulofenestra hampdenensis* and *Discoaster distinctus* Zones, mid Eocene 6/7.
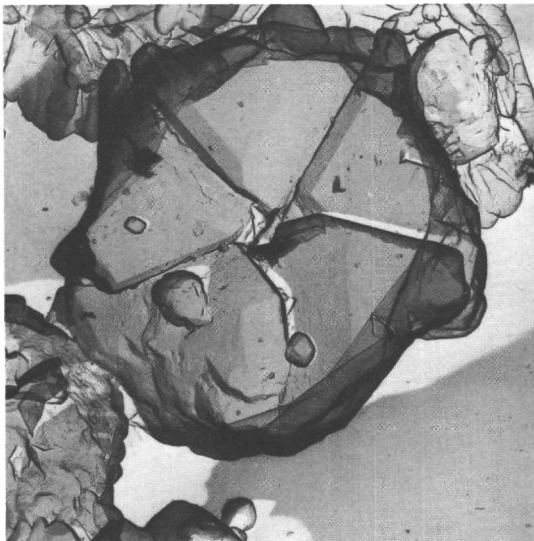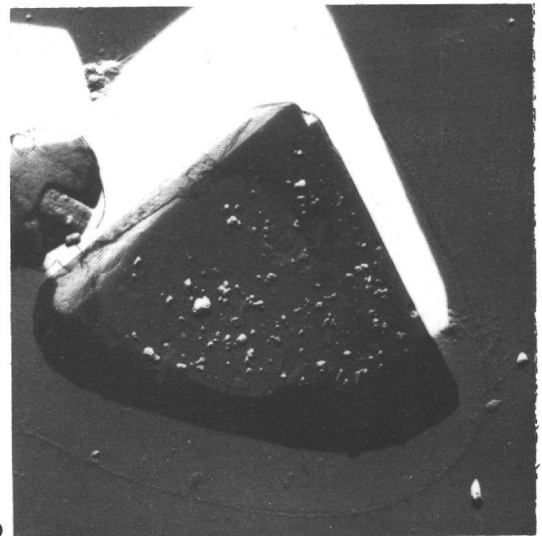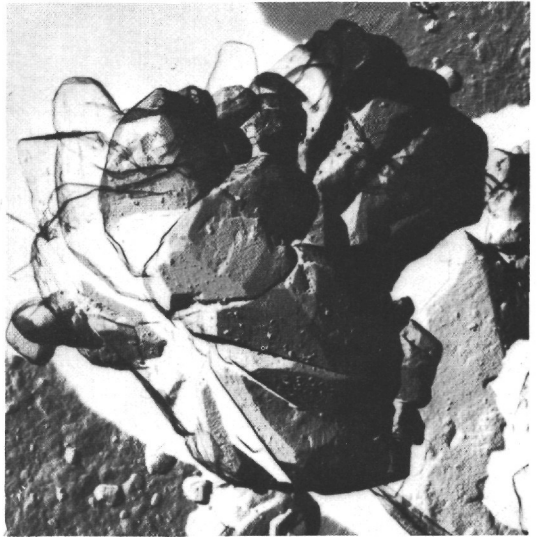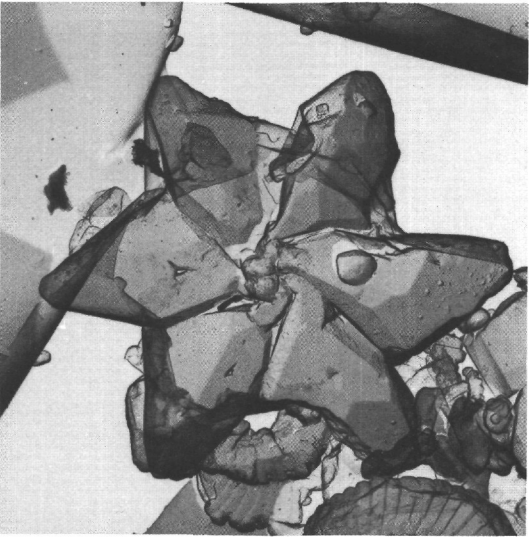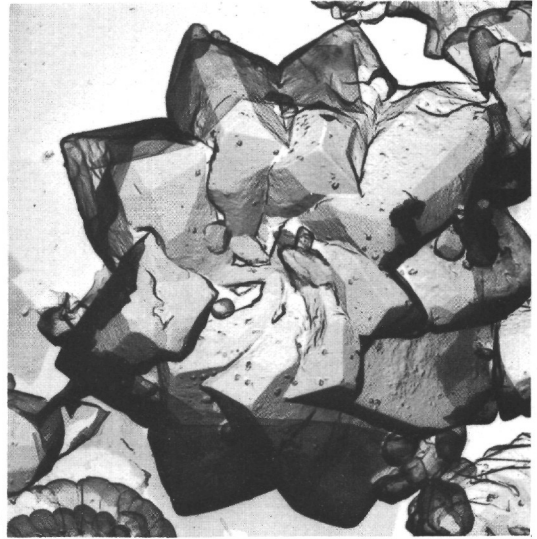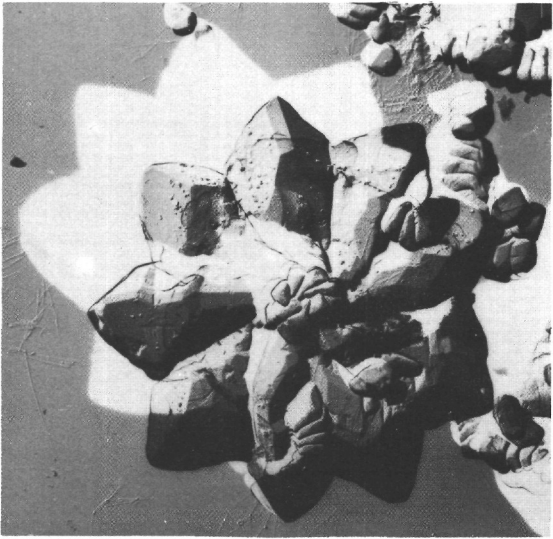
**PLATE 13**
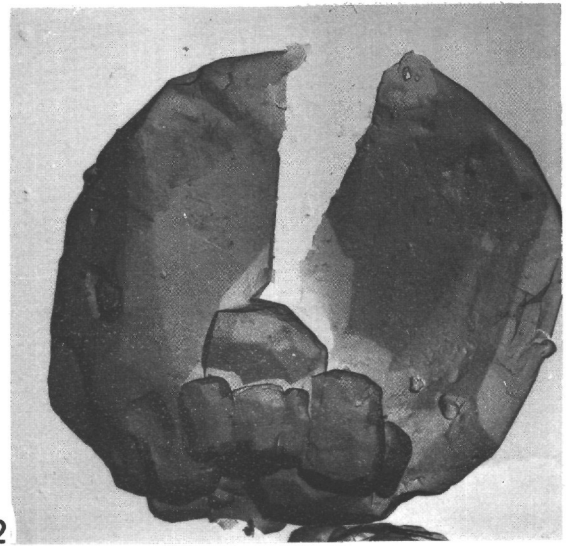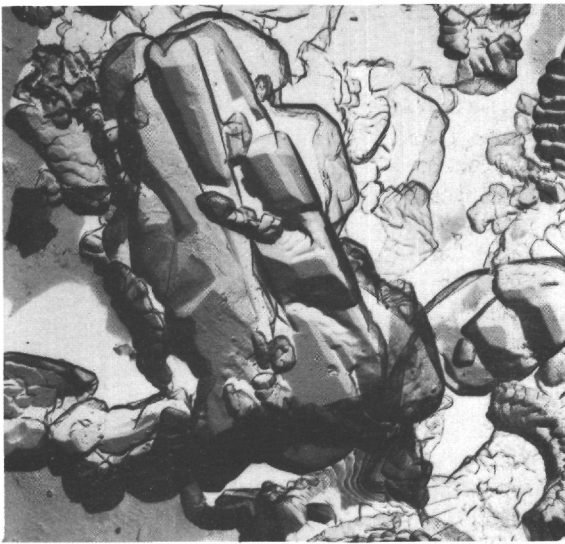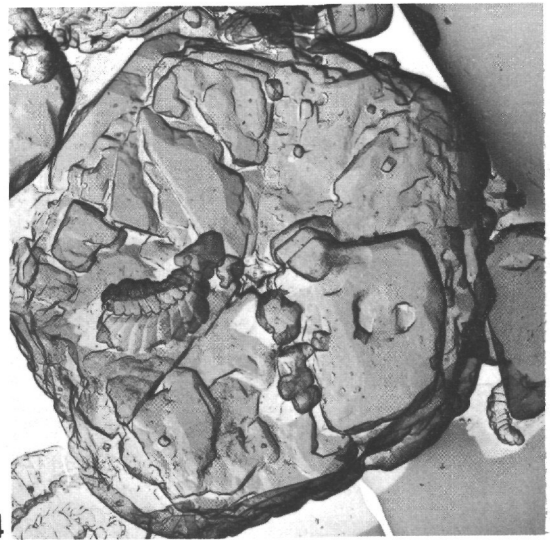
## PLATE 14

Transmission electron micrographs of Discoasteraceae.

Figure 1      *Discoaster barbadiensis* Tan Sin Hok, plan view, 7500X, PEL 2541/3; 207A-20-1, 25 cm, *Chiphragmalithus cristatus* Zone (lower), mid Eocene 3/7.

Figure 2      *Discoaster robustus* Haq, plan view; 7500X, PEL 2539/3; 207A-25-2, 25 cm, *Discoaster lodoensis* Zone, Early Eocene 4/5.

Figure 3      *Discoaster lodoensis* Bramlette and Riedel, plan view; 4800X, PEL 2539/10; 207A-25-2, 25 cm, *Discoaster lodoensis* Zone, Early Eocene 4/5.

Figure 4      *Discoasteroides kuepperi* (Stradner) Bramlette and Sullivan, oblique side view; 7500X, PEL 2539/26; 207A-24-1, 25 cm, *Reticulofenestra dictyoda* Zone (upper), Mid Eocene 1/7.

Figure 5      *Discoaster multiradiatus* Bramlette and Riedel, plan view (note small size of stem); 3700X, PEL 2545/5; 207A-26-4, 100 cm, *Discoaster multiradiatus* Zone, Late Paleocene 1/3.

Figure 6      *Discoaster multiradiatus* Bramlette and Riedel, plan view (opposite side to Figure 5); 7500X, PEL 2541/15; 207A-26-4, 100 cm, *Discoaster multiradiatus* Zone, Late Paleocene 1/3.

PLATE 14
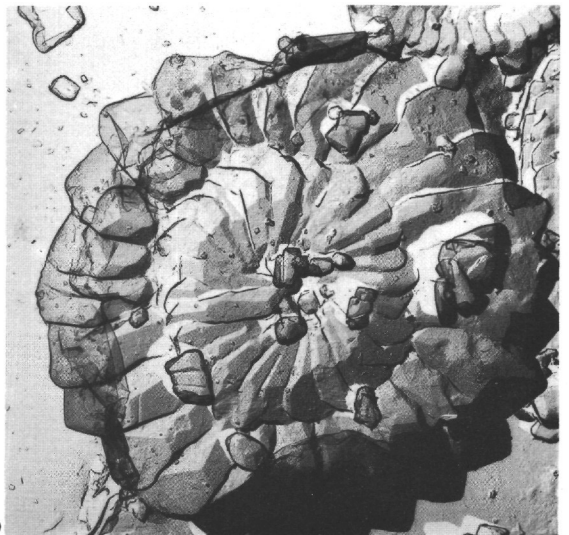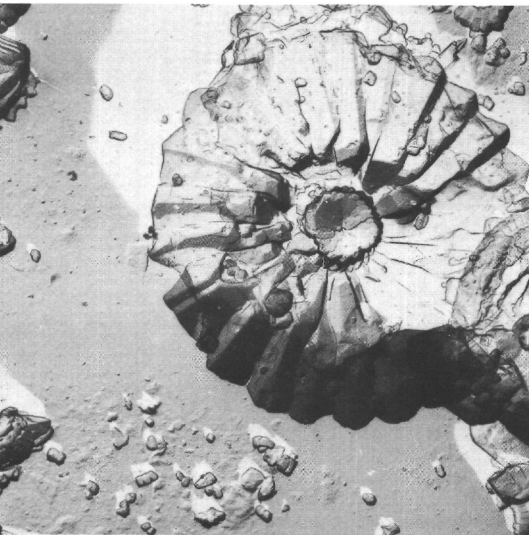
## PLATE 15

Transmission electron micrographs of Fasciculithaceae,
Sphenolithaceae and Thoracosphaeraceae.

Figure 1    *Fasciculithus* aff *tympaniformis* Hay and Mohler, side view (note convexity at both ends); 10000X, PEL 2541/25; 207A-26-4, 100 cm, *Discoaster multiradiatus* Zone, Late Paleocene 1/3.

Figure 2    *Fasciculithus tympaniformis* Hay and Mohler, side view; 10000X, PEL 2541/20; 207A-26-4, 100 cm, *Discoaster multiradiatus* Zone, Late Paleocene 1/3.

Figure 3    *Sphenolithus* sp., oblique side view; 10000X, PEL 2541/33; 207A-26-4, 100 cm, *Discoaster multiradiatus* Zone, Late Paleocene 1/3.

Figure 4    *Thoracosphaera*? sp. cf *T. prolata* Bukry and Bramlette, side view (compare with Plate 1, Figure 5); 2600X, PEL 2539/15; 207A-25-2, 25 cm, *Discoaster lodoensis* Zone, Early Eocene 4/5.

Figure 5    *Thoracosphaera* sp. cf *T. operculata* Bramlette and Martini, side view of damaged nannosphere; 3700X, PEL 2545/1; 207A-26-4, 100 cm, *Discoaster multiradiatus* Zone, Late Paleocene 1/3.

Figure 6    *Thoracosphaera* sp. cf *T. operculata* Bramlette and Martini, oblique proximal view of nannosphere fragment; 7500X, PEL 207A-26-4, 100 cm, *Discoaster multiradiatus* Zone, Late Paleocene 1/3.

**PLATE 15**